A Roadmap for Production of Cement and Concrete with Low-CO_2 Emissions

Jannie S.J. van Deventer[1,2], Claire E. White[3], Rupert J. Myers[4]

[1] Zeobond Pty Ltd, P.O. Box 23450, Docklands, Victoria 8012, Australia.
ORCID 0000-0001-7783-9398
Email: jannie@zeobond.com
[2] Department of Chemical Engineering, University of Melbourne, Victoria 3010, Australia
[3] Department of Civil and Environmental Engineering, Andlinger Center for Energy and the Environment, Princeton University, Princeton, New Jersey, U.S.A.
ORCID 0000-0002-4800-7960
Email: whitece@princeton.edu
[4] Department of Civil and Environmental Engineering, Imperial College London, SW7 2AZ, London, U.K.
ORCID 0000-0001-6097-2088
Email: r.myers@imperial.ac.uk

Abstract

This review will show that low-CO_2 cements can be produced to give superior durability, based on a sound understanding of their microstructure and how it impacts macro-engineering properties. For example, it is essential that aluminium is available in calcium-rich alkali-activated systems to offset the depolymerisation effect of alkali cations on C-(N)-A-S-H gel. The upper limit on alkali cation incorporation into a gel greatly affects mix design and source material selection. A high substitution of cement clinker in low-CO_2 cements may result in a reduction of pH buffering capacity, hence susceptibility to carbonation and corrosion of steel reinforcement. With careful mix design, a more refined pore structure and associated lower permeability can still give a highly durable concrete. It is essential to expand thermodynamic databases for current and prospective cementitious materials so that concrete performance and durability can be predicted when using low-CO_2 binders. Cationic copolymer and amphoteric plasticisers, when available commercially, will enhance the development of alkali-activated materials. The development of supersonic shockwave reactors will enable the conversion of a wide range of virgin and secondary source materials into cementitious materials, replacing blast furnace slag and coal fly ash that have dwindling supply. A major obstacle to the commercial adoption of low-CO_2 concrete is the prescriptive nature of existing standards and design codes, so there is an urgent need to shift towards performance-based standards. The roadmap presented here is not an extension of current cement practice, but a new way of integrating fundamental research, equipment innovation, and commercial opportunity.

Keywords

Alkali-activated material
Cementitious materials
Commercialisation
Durability
Standards
Thermodynamic modelling

Graphical Abstract

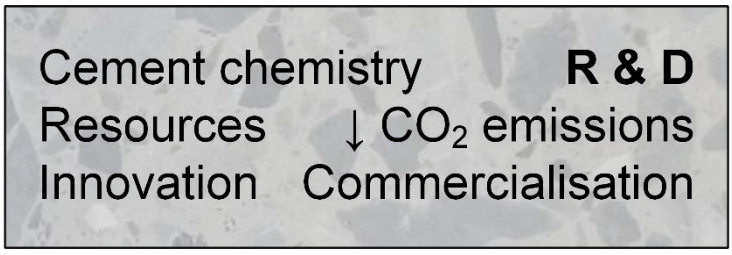

Abbreviations

AAFA	Alkali-activated fly ash
AAGBS	Alkali-activated ground granulated blast furnace slag
AAM	Alkali-activated materials
AAMK	Alkali-activated metakaolin
AFm	Aluminate ferrite monosulphate
AFt	Aluminate ferrite tri-sulphate
ASR	Alkali silica reaction
BFRP	Basalt fibre reinforced polymer
CAC	Calcium aluminate cement
C-(N,K)-(A)-S-H	Calcium (alkali) (alumino)silicate hydrate
C-A-S-H	Calcium aluminium silicate hydrate
C-S-H	Calcium silicate hydrate
C_2S	Dicalcium silicate
DFT	Density functional theory
EESS	Electrically-enhanced supersonic shockwave reactor
FA	Coal fly ash
GBS	Ground granulated blast furnace slag
GDP	Gross Domestic Product
LC^3	Calcined clay limestone cements
LDH	Layered double hydroxide
MCL	Mean chain length
N-A-S(-H)	Alkali aluminosilicate hydrate
NMR	Nuclear magnetic resonance
OPI	Oxygen Permeability Index
PC	Portland cement
PCE	Polycarboxylate ethers
PDF	Pair distribution function
SCM	Supplementary cementitious material
TEM	Transmission electron microscopy

Statement of Novelty

Numerous papers have been published on blended cements and alkali-activated materials with the aim to reduce CO_2 emissions. However, the obstacles to commercialise these cements have not been properly identified before. Also, the gaps in the existing research on low-CO_2 cements are not evident, unless commercial imperatives are considered as well. Unlike many other review papers on cementitious materials, the aim here is to develop a roadmap for future research and the commercial production of low-CO_2 cements. Novel technology coupled with a re-interpretation of the literature will underpin the development of a new value chain for cementitious materials. Moreover, it is

shown that the chemistry of blended cements and that of alkali-activated materials should be conceptualised as a continuum.

Introduction

The world population is predicted to grow by ~3 billion people by 2100, up from ~8 billion in 2019, with this growth arising from low-and-middle income countries [1]. Concomitant increasing demand for basic services like shelter, transportation and sanitation networks, and information technology, will undoubtedly drive production of more construction materials at a similarly massive scale, especially those used in buildings, transport, and infrastructure. Global construction output is expected to exceed USD 15 trillion by 2030 with China, the US and India accounting for 57% of all global growth. Also, global construction growth is expected to outpace that of global GDP by over one percentage point [2], so with construction contributing about 10% of global GDP, demand for cement and concrete will continue to grow.

Concrete as the main construction material is relatively inexpensive to produce due to the abundance of its components, i.e. aggregate consisting of crushed rock like granite and quartz, and sand, as well as cement and water as the binder. The production of cement is ubiquitous due to the abundance of its source materials, i.e. limestone and clay. Concrete has relatively high durability, has good aesthetics, and is simple to use, so it will almost certainly continue to be the preferred construction material. The global annual cement consumption in 2016 was 4.13 Gt and it is expected to grow to 4.68 Gt/year by 2050 [3], making it one of the most widely used commodities.

Today the cement industry is the third largest industrial energy consumer and its production accounts for 5-8% of global anthropogenic CO_2 emissions, which corresponds to 3-6% of anthropogenic greenhouse gas emissions in CO_2-eq. [3,4]. The CO_2 emissions from the production process originate as fuel-related CO_2 from fossil fuel combustion in order to generate thermal energy, and as CO_2 from the decomposition of limestone in the calcination process. Any attempt to reduce the high CO_2 emissions from cement clinker production is constrained by the decomposition of limestone, so the preferred strategy is to replace clinker in cement blends. Ellis et al. [5] proposed electrochemical calcination that produces a concentrated gas stream from which CO_2 may be separated. Even if the global cement industry achieves its own emissions targets, cement-related emissions may contribute an alarming 20% of global carbon emissions by 2050 [6]. Clearly, there is a need to change cement production practice in order to reduce CO_2 emissions. In addition to cement production, work is being done to reduce CO_2 emissions across the cement cycle, including quarrying, the production and transportation of concrete, the management of end-of-life materials, recycling, optimisation of concrete structural design to minimise cement consumption, and enhanced durability to extend the life of structures and hence minimise cement consumption. The use of alternative fuels such as municipal solid waste is an integral part of the modern cement production process, and has contributed substantially to recycling of residue and CO_2 reduction[7]. Although expensive and highly energy intensive, the capture and geological storage of CO_2 is viewed as a future technology to substantially reduce CO_2 emissions from clinker production. For this to succeed, industrial and climate policies need to be aligned, in particular to support early movers that will otherwise become uncompetitive [3,6].

Numerous papers have been published on the chemistry of low emissions cements, so it is not the aim here the reproduce those perspectives. In particular, the use of coal fly ash (FA), ground granulated blast furnace slag (GBS) and calcined clay as supplementary cementitious materials (SCMs) in blended Portland cement (PC) has been reviewed extensively [8-11]. Similarly, the use of alkalis to activate precursors, mainly industrial secondary materials, has been reviewed extensively [12-15]. There has also been increasing focus on calcined clay limestone cement (LC^3) binders to reduce CO_2 emissions by replacing 50% cement clinker [16].

Despite detailed research on the microstructure of such binders and claims that they are durable under aggressive exposure conditions, these binders have not been applied widely. This review will analyse the reasons for the slow adoption of 'low-CO_2 binders', including supply chain constraints, cement and concrete standards, structural design codes, questions about durability and the lack of suitable admixtures. Here, 'low CO_2 binders' are defined as having CO_2 emissions significantly lower than conventional blended PC. A roadmap will be developed for a new value chain to convert unexploited virgin materials and industrial by-products to cement and concrete with low CO_2 emissions. By reviewing recent research, it will be shown that low CO_2 binders can give superior durability and macro-engineering performance when using a deep understanding of their microstructure. Gaps in the existing knowledge on low-CO_2 binders will be identified, and it will be shown that such gaps also exist for more conventional binders. PC blends, AAM and LC^3 will be considered as a continuum for the purpose of phase formation and thermodynamic prediction of material properties.

Thermodynamic Prediction of Cementitious Performance

Fundamental aspects of performance

Cementitious product performance is underpinned by properties of the cement binder, i.e., 'matrix'. The matrix is a complex composite of air, aqueous solution ('pore solution'), and various solid phases, each of which have distinct material properties and shape. For example, calcium (alkali) (alumino)silicate hydrate (C-(N,K-)(A-)S-H) is a relatively stiff, stable, and plate-like solid phase that precipitates readily in high pH systems rich in Ca and Si [17]. These desirable properties are key to the dominance of C-(N,K-)(A-)S-H in PC based binders. These binders are designed to stabilise this phase at the right time, and in high amounts, to create a dimensionally constant and dense matrix for many engineering applications of cementitious products [18].

Cementitious matrix properties are commonly distinguished into 'physical' and 'chemical': the former provides performance through (macro)shape/(micro)structure and mechanics, and the latter provides performance through the chemistry of the system. The key physical properties are related to shape, since the matrix (and its interface with aggregate particles) has lower resistance to diffusion than aggregate particles, and is itself a solid-gas composite (where gas is the least dense, stiff, and strong phase in cement-based materials). Chemical properties include the types, (molecular) structures, and chemical compositions of phases (solid, aqueous, gaseous) and their constituents present in the matrix. They are important in the provision of durable concrete cover for steel reinforcement, where reactive transport phenomena underpin service life [19].

Physical and chemical properties are inherently related, since, e.g., different solid phases (with different chemistry) have distinct shape and (molecular) structure. There are many possible solid phases in cementitious systems, with their occurrence depending upon the chemistry of their surroundings, and the matrix having characteristic ordering over several decades of length units, from nanometres (individual phases) to microns (matrix-aggregate interaction). This multi-scale and temporal nature of the matrix increases the difficulty of characterising its components [20]. However, chemical properties are arguably more fundamental than mechanical properties. The way in which source materials are processed into cementitious products dictates phase formation, e.g., through a specified mix design and curing conditions, which subsequently affects their distribution and the resulting shape of the cementitious matrix [21]. For this reason, we focus here on prediction of chemical properties of cementitious matrices through thermodynamic modelling, and provide perspectives on how this approach may be extended to provide a basis for coupled physico-chemical property and performance prediction of cementitious materials in general.

Thermodynamic modelling

Thermodynamic modelling refers to methodology that uses thermodynamics to predict phase and component speciation under (near-)equilibrium conditions (Figure 1) [22]. Its application to systems involving formation, persistence, and degradation of cementitious matrices focuses calculating liquid-solid equilibrium, since gaseous phase chemistry usually does not contribute to matrix properties and performance. Matrix properties have been investigated comprehensively for Portland cement systems for more than two decades [23-26], whereas matrix performance is less well studied [27,28]. This represents a significant research gap, especially with respect to durability as a measure of performance. Here, more experimental durability studies involving thermodynamic modelling are desired, to better explain experimental observations. For this to occur, reliable and comprehensive thermodynamic databases are needed. This desired situation involves a feedback loop in which experimental durability research and thermodynamic database development should be conducted in tandem. It is reflected by the loop in Figure 1, which is a conceptual diagram summarising the thermodynamic modelling method.

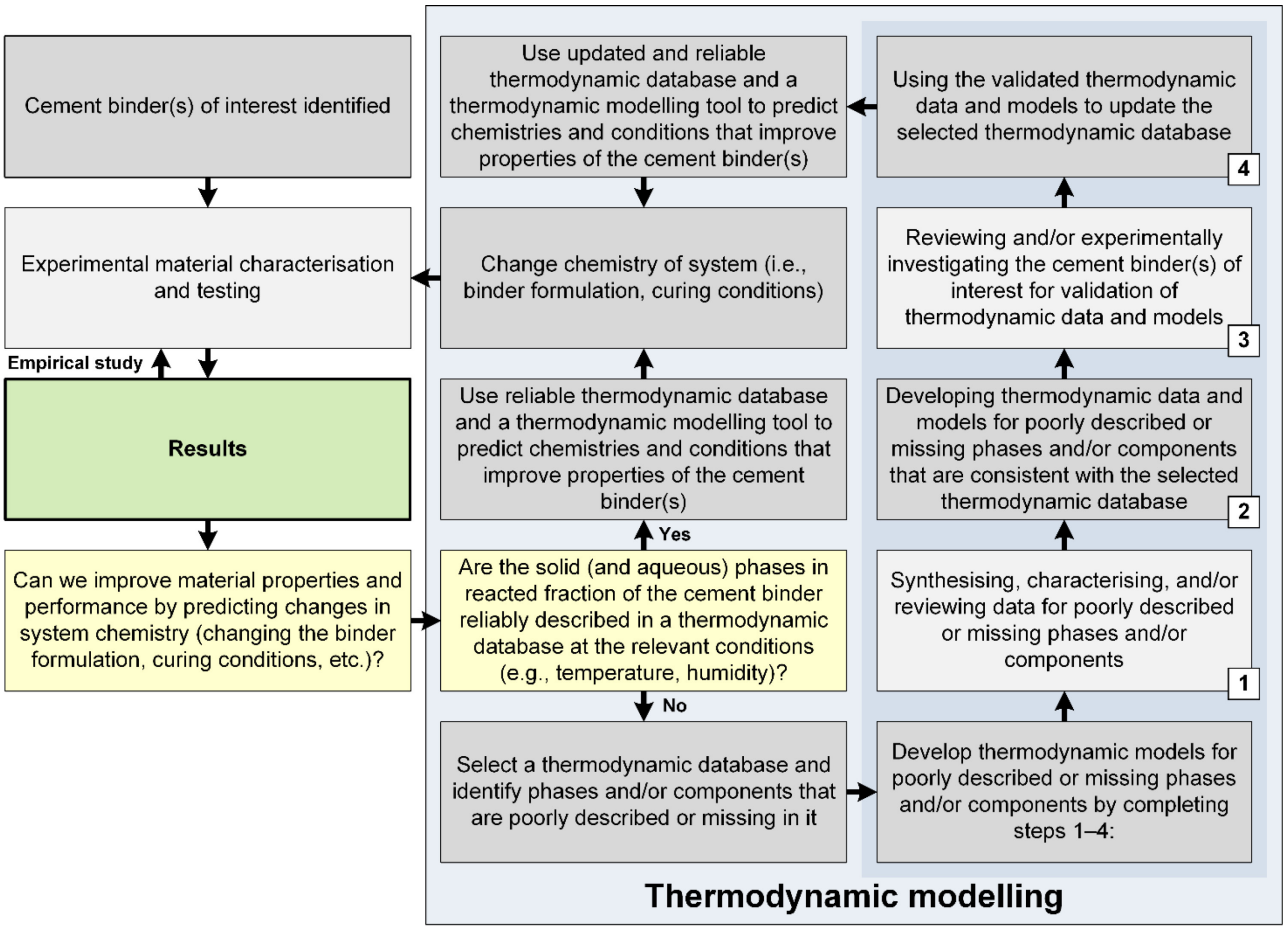

Figure 1. Conceptual flow diagram of thermodynamic modelling

Thermodynamic modelling (blue box, Figure 1) uses thermodynamic properties such as the Gibbs free energy (ΔG, J mol^{-1}), enthalpy (ΔH, J mol^{-1}), entropy (S, J mol^{-1} K^{-1}), and equilibrium constants that relate to the Gibbs free energy of reaction ($\Delta_r G$) through eq.(1). If a dissolution reaction is specified, these equilibrium constants are called solubility constants, K_s:

$$\Delta_r G^{\$} = -RTln(K_s) \quad (1)$$

where R is the universal gas constant (8.3145 J mol^{-1} K^{-1}), T is temperature (K), and $^{\$}$ denotes that the property is quantified at the reference state. The reference state is commonly 298.15 K and 1 bar for solids, and unit activity in a hypothetical one molal (i.e., mol kg^{-1}) solution referenced to infinite dilution for solutions [29]. Sometimes the Gibbs free energy is modelled in a 'Gibbs free energy minimisation' approach; alternatively, solubility constants may be modelled in a 'law of mass action' approach [30]. The selection of approach ('thermodynamic modelling tool' in Figure 1) is superficial; what is important is that the equilibrium condition is obtained, that is, at equilibrium the system experiences no driving force to change. This occurs when the chemical potential (μ, J mol^{-1}, where $\mu_i = \mu_i^{\$} + RT\ln(a)$, a_i is the activity of component i, and the other symbols are defined above), temperature (T), and pressure (P) are equal in every phase, which occurs when the Gibbs free energy is minimal [31]. Here, 'stability' refers to this equilibrium condition, i.e., a phase is stable when it constitutes the system in which the Gibbs free energy is minimal.

A useful test for stability in cementitious systems involves calculating the saturation index (SI) (eq.(2)):

$$SI_i = \log_{10}\left(\frac{IAP_i}{K_{s,i}}\right) \tag{2}$$

where IAP is the ion activity product of component i and the other symbols are defined above. The IAP and solubility product refer to the same dissolution reactions, and SI_i denotes the saturation state of the system with respect to component i: $SI_i > 0$ indicates supersaturation (precipitation); $SI_i = 0$ indicates saturation; and $SI_i < 0$ indicates undersaturation (dissolution). Cementitious systems have relatively high ionic strengths of $I \sim 0.5$ mol kg^{-1} in PC binders and typically $I = 1$-3 mol kg^{-1} in AAM [32,33]. Therefore, aqueous component activities are usually modelled using extensions of the Debye-Hückel equation, e.g., eq.(3) (the Helgeson extension) [29]:

$$\log_{10}(\gamma_i) = \frac{A_\gamma z_i^2 \sqrt{I}}{1 + \dot{a} B_\gamma \sqrt{I}} + b_\gamma I + \log_{10}\left(\frac{x_{jw}}{X_w}\right) \tag{3}$$

where γ_i (–) is the activity coefficient of component i, A_γ (kg$^{1/2}$ mol$^{-1/2}$) and B_γ (kg$^{1/2}$ mol$^{-1/2}$ Å^{-1}) are parameters that depend upon solvent properties and temperature, z_i (–) is the charge of component i, $\dot{a}$ (Å) is the average distance of closest approach of two ions of opposite charge, I is the ionic strength (mol kg^{-1}), b_γ (kg mol^{-1}) is the extended term, x_{jw} (mol) is the amount of water, and X_w (mol) is the total amount of aqueous phase components. Cementitious matrices are highly multicomponent systems; therefore, use of an extended Debye-Hückel equation is arguably preferable over other approaches that would require data for many specific interaction parameters, e.g., Pitzer [34,24]. Nevertheless, improvements to aqueous component activity modelling to improve reliability at high ionic strength and in highly multicomponent systems, including both inorganic and organic components, is desirable.

Cementitious matrices comprise many aqueous components and several stable solid phases, and usually there are numerous others (e.g., over sixty in Cemdata18 [35]) that are potentially stable depending upon processing conditions and environmental exposure. A thermodynamic database contains thermodynamic models, comprising thermodynamic property data (ΔG, ΔH, S, etc.), for phases and constituents. All potentially stable phases should be included in the thermodynamic database used, in addition to an equilibrium solver ('thermodynamic modelling tool' in Figure 1), to ensure model reliability. Thermodynamic models can be relatively simple, e.g., employing ideal

mixing of thermodynamic properties, or more complex (e.g., employing non-ideal mixing conditions) [36-38].

Currently, the most comprehensive databases for cementitious systems [35,39] focus on phases relevant to PC binders, although more recently thermodynamic models for alkali-activated materials (AAM) have been developed and included [37,40]. These thermodynamic databases, coupled with information of the reactivities of PC and various SCMs in cementitious systems [41,42], have been used mainly to describe PC hydration. Overall, thermodynamic modelling has enabled chemical properties of PC-based binders (from low to high substitution of PC for SCMs) and some AAM (e.g., alkali-activated GBS (AAGBS)) to be predictively optimised as functions of raw material type and chemistry with good reliability. It has provided a fundamental and rational approach to developing cementitious binders with lower embodied CO_2 emissions than ordinary PC binder. As outlined in Figure 1, current thermodynamic databases for cementitious materials are being extended to include thermodynamic property data for phases relevant to other systems [43,44], however, at present many data gaps remain. Filling these data gaps (through steps 1-4 in Figure 1) will facilitate development of low CO_2 cementitious binders that exploit underutilised resources.

The dominant solid phase in PC binder, C-(N,K-)(A-)S-H (simply referred to as C-S-H due to the relatively low alkali and Al content in PC systems), is usually accompanied by several solid phases: portlandite, ettringite, Mg-Al and Ca-Al layered double hydroxide (LDH) phases (hydrotalcite, AFm), Al,Fe-Si hydrogarnet, and calcite (in the presence of CO_2, e.g., curing in air and/or with limestone in the mix design) [25]. Many of these solid phases form solid solutions, and reliable thermodynamic models for these are generally available [35]. However, reliable thermodynamic models for potentially stable solid phases in low- and non-PC systems are less well developed: a notable example is the zeolite-like alkali aluminosilicate (hydrate) (N-A-S(-H)) gel that stabilises in low-Ca AAM [45]. Development of reliable thermodynamic models for these phases is a key research need in the prediction of cementitious material property and performance.

Chemistry-Structure-Property Relationship

This section outlines important links that exist between the fundamental chemical attributes of alkali-containing cements and in-field performance. By understanding how the chemistry influences the (i) type and amount of solid phases, (ii) reaction mechanisms and kinetics, (iii) pore network and (iv) pore solution chemistry, the durability of the cement can be uncovered. Figure 2 provides a comprehensive overview of these links between chemistry and durability, and the individual areas are outlined below.

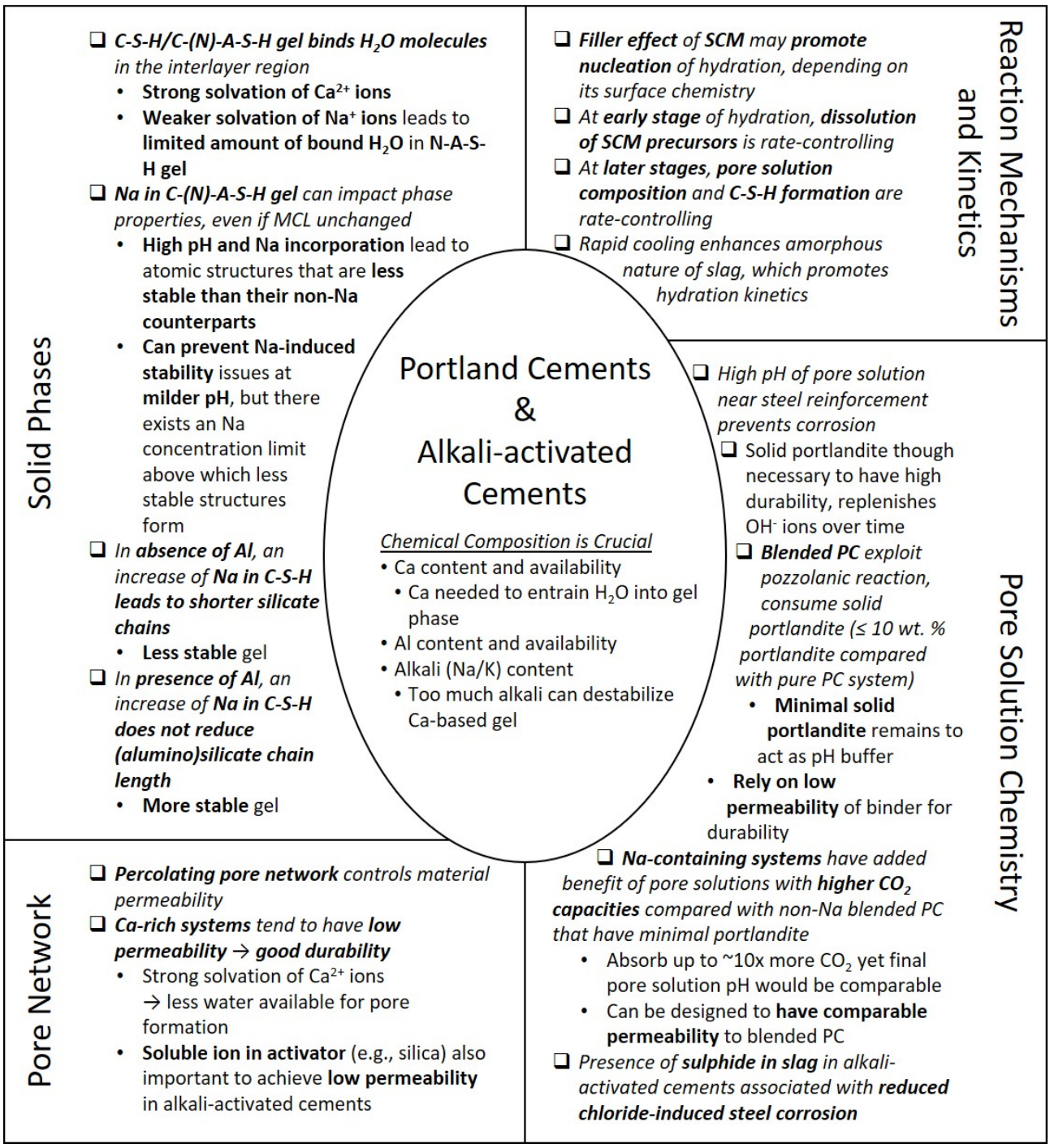

Figure 2. Schematic overview of the link between chemical composition of alkali-containing cements and durability by considering (i) the solid phases, (ii) reaction mechanisms and kinetics, (iii) pore network and (iv) pore solution chemistry.

Solid Phases

As mentioned previously, the main binder phase providing mechanical strength in PC-based concrete is C-S-H gel, and when SCMs such as FA, GBS, and calcined clays are incorporated in an effort to improve properties and reduce CO_2 emissions [46], the chemistry and structure of the gel are augmented [47]. A significant amount of research has been performed on the impact of GBS and FA on the structure of C-S-H gel [48,49,10], where it is clear that Al is incorporated into the dreierketten silicate chains, specifically in bridging q^2 sites leading to a C-A-S-H gel [50]. The transition from Q^1 and Q^2 silicate units in C-S-H to Q^1 and Q^2 silicates and q^2 aluminate in C-A-S-H

has been associated with an increase in gel stiffness, as measured by nanoindentation [51,52]. Hence, it is clear that SCMs in PC have had a positive effect on the resulting C-S-H-type gel in terms of its attributes and associated properties [9]. A related type of C-A-S-H gel (denoted as C-(N,K)-(A)-S-H) is known to form in AAGBS [53]. Characterisation of this gel using nuclear magnetic resonance (NMR) [54-56,53], transmission electron microscopy (TEM) [54,56], and pair distribution function (PDF) analysis [57-59] has shown that it possesses similar attributes and associated properties to the gels found in PC incorporating Al-rich SCMs (although Q^3 silicate sites are found in AAGBS [53], which are not found in PC-based C-A-S-H).

One area that has remained largely unexplored until recently is how alkalis, such as Na and K, affect the chemical and physical properties of C-A-S-H gel, an area that is directly relevant for Ca-rich cement systems such as AAM incorporating PC powder, and those based on AAGBS. Historically such alkalis have been avoided due to the possible alkali silica reaction (ASR, also often referred to as the alkali aggregate reaction, AAR) known to occur when reactive aggregates, calcium, alkalis, and an external water source are present [60-62]. Previous research has shown that AAM concretes are less susceptible to ASR, perhaps due to their lower Ca content [63], though the reasons for this improved behaviour are still being investigated [64-66]. Thermodynamic modelling, using concepts described above such as the saturation index, is playing a key role in advancing understanding of ASR [63,67]. Therefore, a shift in perspective is needed within the concrete industry to allow for alkali-containing concretes. Nevertheless, interest in using ground recycled waste glass powder as a SCM for PC-based concrete is growing in the construction industry [68,69]. This SCM tends to be rich in SiO_2 and Na_2O, with the exact oxide composition dependent on the types of glass making up the waste stream [70].

Initial research on the influence of alkalis on C-S-H gel showed that it is possible to synthesise C-(N)-S-H [71] and C-(N)-A-S-H gels [72-76], where alkalis were directly taken up by the precipitating gel and incorporated into the gel structure [72]. Solubility measurements of the resulting gels showed that the alkali-containing gels possessed a similar solubility to C-A-S-H [73], indicating that these gels should perform similarly in a given chemical environment, however, such analyses were performed on systems that were synthesised in hydroxide solutions up to 1.0 M, where higher hydroxide concentrations may lead to a different outcome. At the macroscopic level, mechanical testing of AAGBS (i.e., those containing C-(N)-A-S-H gel) and pure PC paste (C-S-H gel) has revealed similar mechanical properties [55,77-79], which is partially attributed to the mechanical properties of the gels together with similar pore structures [80,81]. Hence, it is clear from the literature that alkali-incorporation into Ca-rich cements, such as AAGBS, leads to a binder gel with comparable chemical and mechanical properties to a PC binder gel.

Moving forward, the ability to be able to predict gel performance based on chemical composition would not only enable the exploration of a wide variety of SCMs, but would also allow for the chemistry to be pushed beyond what is currently possible in experiments and in-field trials and to find the composition limits beyond which the material attributes are no longer beneficial. Computer simulations, and particularly *ab initio* calculations, are now used throughout the materials science community to predict material properties and performance [82-84], and such calculations have been carried out on PC and AAM binders, albeit to a limited degree [85-89]. This is due to the disordered nature of the C-S-H gel together with the existence of multiple reacting clinker phases and secondary products. Although AAGBSs possess fewer distinct phases than hydrated PCs, the amorphous nature of the GBS precursor together with the disordered C-(N)-A-S-H gel and secondary products (such as LDHs) complicates the simulation approach. Thermodynamic information, such as the energy and enthalpy of formation can be obtained from density functional theory (DFT) calculations, and therefore details on relative phase stability and susceptibility to degradation can be determined. However, such extensive analyses have yet to be performed.

Özçelik and White used the model 14Å tobermorite structure as the crystalline analogue of C-S-H gel to study the impact of alkalis and Al substitution on the thermodynamics of this phase [89]. The use of a crystalline structure was necessary owing to (i) the lack of detailed structural representations of C-S-H gel that have been carefully optimised using DFT calculations and are in agreement with the experimental data available in the literature, and (ii) the need for a relatively small system size (i.e., < 400 atoms) for the computationally-intensive DFT calculations at a high level of precision. By substituting an interlayer Ca atom with one Na (or two Na^+) it was found that the structure was less stable (i.e., it had a higher energy compared with 14 Å tobermorite) as seen in Figure 3 by comparing "14Å Tobermorite" with "Ca→Na", as was the case for the same substitution along with a bridging Si being replaced by Al (denoted as "CaSi→NaAl" in the figure). However, when the substitution (Ca for Na, or Si for Al) was accompanied by a H atom, the stability of the resulting structure was similar to 14 Å tobermorite (see Figure 3 and the "Ca→Na+H" and "CaSi→NaAl+2H" data). This finding provides important insight on the impact of solution pH on the thermodynamics of the gel, since a high pH (e.g., 13 to 14) would not allow for ample protonation of the sites (i.e., silicate species) adjacent to Na and/or Al, leading to a less stable gel. On the other hand, synthesis of the material under more mild pH conditions may result in a gel with comparable thermodynamic stability. The need for high pH activators, such as NaOH, in AAGBS has historically been reported as a means of kicking off precursor dissolution and therefore obtaining adequate early strength development. However, there can be adverse consequences of the rapid availability of certain elements, such as Al in low-Ca systems, where aluminate species quickly react with ions in solution to form a gel on the surface of reacting particles, thereby limiting additional precursor dissolution and subsequent gel precipitation [90]. Hence, careful control of the rate and location of gel formation is needed, and more research on this topic is necessary. Nevertheless, the findings from the study by Özçelik et al. [88,89] have catalysed research focused on using other approaches to enhance precursor dissolution without resorting to high pH activators (i.e., pH 13 or greater), and therefore, provided that adequate charge-balancing by hydrogen atoms takes place in the C-S-H gel, these new systems appear promising for moving AAM toward lower pH activators.

The aforementioned computational approach has been extended to determine how an increase of the alkali concentration affects gel stability, beyond the alkali concentrations studied experimentally [88]. This information is crucial for PC blended with alkali-containing SCMs (e.g., sodium in waste glass) and systems activated by alkalis (e.g., AAGBS). Moreover, AAM incorporating a small amount of PC (< 10 wt. %) are also of industrial significance, with the results presented here of direct relevance to these alkali-activated PC-containing binders. Özçelik et al. [88] performed DFT calculations and MD simulations on 11Å clinotobermorite (another crystalline analogue for C-S-H gel, specifically involving cross-linking), with the aim of determining the impact of increasing alkali concentration on the stability of the phase. Each interlayer Ca atom was systematically replaced by a Na and H atom until all interlayer Ca atoms were substituted. At each stage of substitution (i.e., alkali concentration) the relative stability of the structure was calculated with respect to 11Å clinotobermorite and are reported here in Figure 4. The results revealed that there is a critical alkali concentration (~0.11 Na/Ca ratio, see Figure 4), beyond which the stability of the gel is adversely affected. This concentration corresponds to a level that is likely realised in most Ca-rich AAM (i.e., a Na/Ca ratio > 0.1 for the gel) [91], although additional research is needed to assess the impact of finite silicate chain length on the relative stability of the structure and, for the experimentally determined Na/Ca ratios for the gel, the amount of alkali adsorbed to gel pore surfaces.

The impact of alkali concentration on the stability of the gel has also been assessed by studying the degree of polymerisation of the C-S-H gel using NMR [72,73] (and more recently PDF analysis [92]). The results clearly show that, in the absence of Al, an increase in alkali concentration leads to a shorter mean chain length (MCL) for the gel [72,73,92], and the possible existence of Q^0 sites

[92]. A shorter MCL means that less siloxanes need to be broken to liberate a silicate monomer, and therefore the gel will be more reactive (i.e., less stable) in an aggressive environment [92]. Nevertheless, when Al is also incorporated into the gel the MCL tends to be similar to C-S-H gel [93]. Hence, there are a number of factors that affect the silicate chains of C-S-H-type gels in PC and AAM systems, and therefore there is the opportunity to tailor the chemical composition of the cement systems to obtain durable (i.e., stable) gels. In particular, with the increase in alkali concentration in cement systems, it is advisable to also have an adequate supply of accessible Al to obtain a durable gel [92].

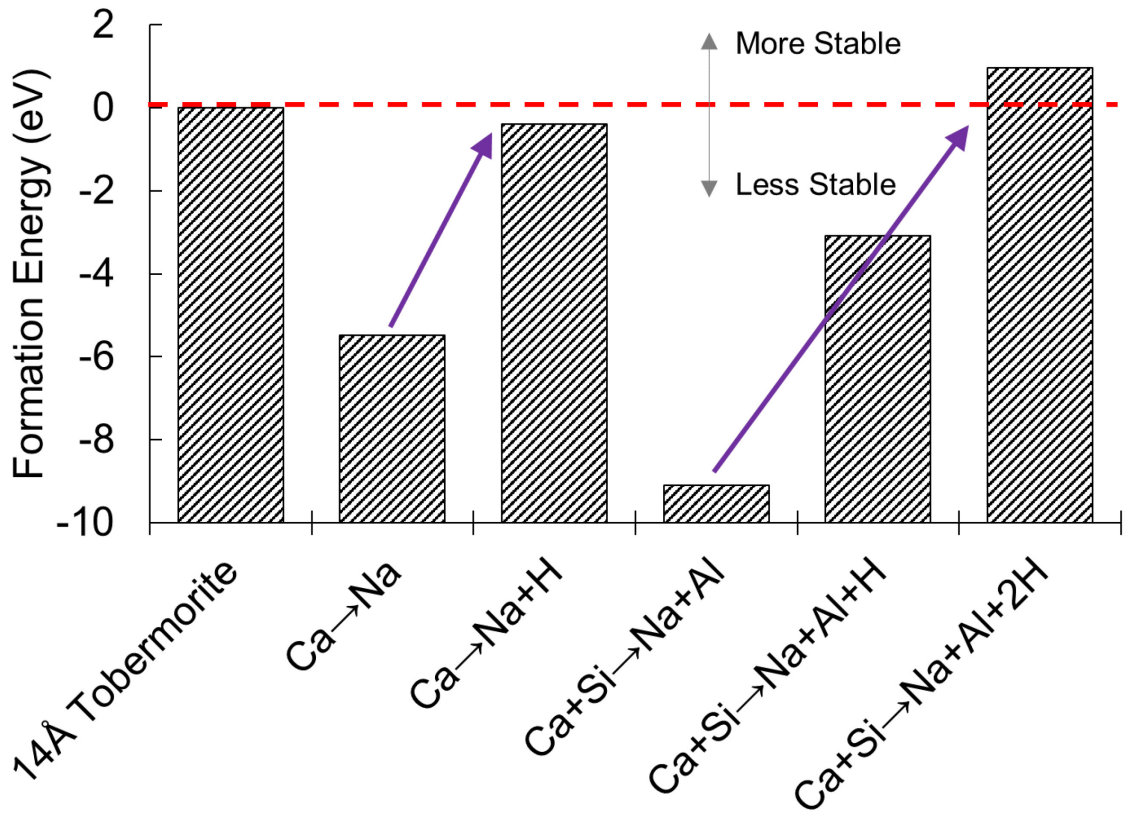

Figure 3. Effect of alkali and Al substitution on the stability of C-S-H gel, modelled using the 14Å tobermorite crystal structure. The stability was assessed by first calculating the cohesive energy of the two respective structures (i.e., before and after substitution) and then taking the difference of these cohesive energies (i.e., the formation energy). A negative formation energy indicates a less stable structure compared with 14Å tobermorite (at 0 eV). The effects of charge balancing were taken into account for certain structures, denoted by the presence of hydrogen atoms after substitution. For example, substitution of Ca for Na+H, together with Si for Al+H in the structure (denoted as "Ca+Si→Na+Al+2H" in figure) leads to a structure that is more stable than the original 14Å tobermorite structure by ~1 eV.

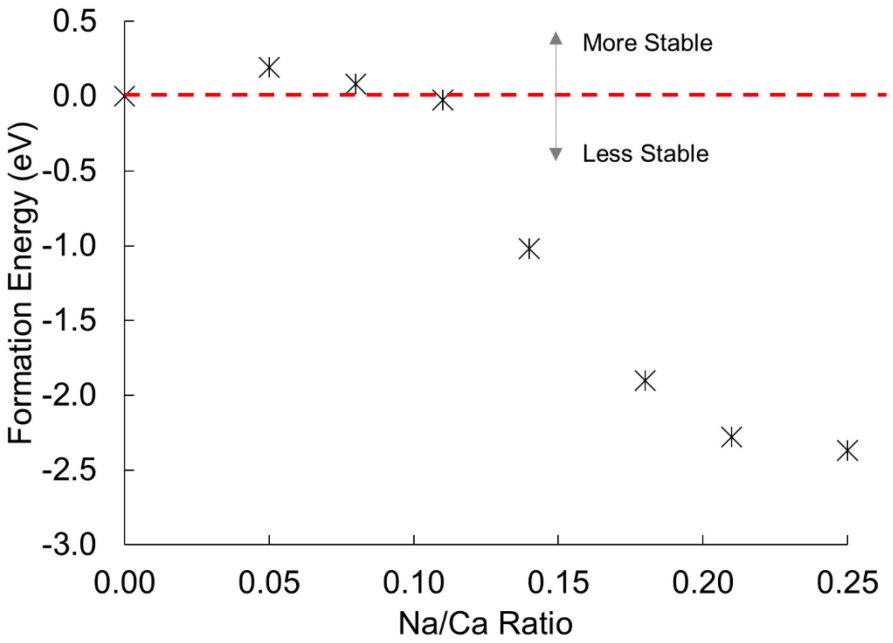

Figure 4. Effect of alkali substitution on the stability of cross-linked C-S-H-type gel, modelled using the 11Å clinotobermorite crystal structure. The stability was assessed by first calculating the cohesive energy of the two respective structures (i.e., before and after substitution) and then taking the difference of these cohesive energies (i.e., the formation energy). A negative formation energy indicates a less stable structure compared with 11Å clinotobermorite (at 0 eV). For all substitutions, each Ca replacement by an Na was accompanied by the inclusion of a H atom (i.e., to maintain a charge-balanced structure). A relatively low amount of Na substitution in the structure does not affect stability, but above a Na/Ca ratio of ~0.11 the stability of the structure is adversely affected. Note that a Na/Ca ratio of 0.25 corresponds to all interlayer Ca atoms being replaced by Na.

The most significant augmentation of the gel is found when transitioning away from Ca-rich systems (containing C-S-H-type gel) to Ca-poor systems [94-98], such as those based on alkali-activated metakaolin (AAMK) and alkali-activated class F fly ash. The alkali aluminosilicate hydrate gel (often referred to as N-A-S(-H) gel where Na is the alkali) is a three-dimensional aluminosilicate (c.f. the layered C-S-H consisting of silicate chains) where both the silicate and tetrahedral aluminate units are fully polymerised (denoted as Q^4 and q^4, respectively) [97]. Another key difference between N-A-S(-H) and C-S-H-type gels is the amount of chemically bound water tied up within the gel. For C-S-H-type gels, chemically bound water is found in the interlayer regions of the gel and as hydroxyl units [99]. On the other hand, for N-A-S(-H) gel the only chemically bound water exists as hydroxyl units, of which there are relatively few [100]. The ability to chemically incorporate water into the gel has a profound impact on the durability of the cement, since the more water within the gel leads to less water ending up in pores, and therefore a more refined pore structure (i.e., smaller pores making up the pore network), as discussed below.

The reason for this difference in amount of chemically bound water in C-S-H-type and N-A-S(-H) gels is likely due to the strength of solvation of the various ions in solution and their speciation at elevated pH. In terms of solvation, the stronger the free energy of solvation, the less likely it will give up the water molecules when partaking in bonding events. Although this is a somewhat simplified viewpoint, since the free energies of the various bonding configurations would need to be taken into account, and therefore even for an ion that is strongly solvated, there may be a driving force for it to give up its water molecules; this comparison may shed light on the different behaviour of Ca and Na ions. The solvation free energy for a Ca ion is ~4-5 times stronger than that for a Na ion [101], and therefore Ca ions hold onto water molecules much more strongly than Na ions and are less likely to give up their water molecules when being incorporated into the gel. Furthermore, at high pH (e.g., pH of ~13-14) it is known that apart from the hydrated Ca ion (e.g.,

$Ca(H_2O)_n^{2+}$, where n is the number of water molecules solvating the ion), both $Ca(OH)^+$ and $Ca(OH)_2$ species are present in solution [102]. Such speciation will likely lead to the incorporation of hydroxyls into the gel. On the other hand, Na ions readily dissociation from hydroxyl units in an aqueous solution due to the high solubility of NaOH (compared with $Ca(OH)_2$) [103] and therefore there is no driving force for Na-induced hydroxyl incorporation into the N-A-S(-H) gel. Hence, there are several reasons for the incorporation of water molecules and hydroxyls into C-S-H-type gels, and not N-A-S(-H) gels, attributed to the presence of Ca and behaviour of Ca ions.

Pore Network

As alluded to above, there are clear differences in terms of water and hydroxyl incorporation in C-S-H-type and N-A-S(-H) gels that are dependent on the Ca ions in the system. This behaviour, together with the amount of water used during mixing, has a large effect on the resulting connected pore structure of the cementitious binder. It is well known that very mature hydrated PC (with a water-to-cement ratio of 0.5) consists of a connected pore structure dominated by pores that are ~5-10 nm in size [104], which is similar to the pore size distribution of 28-day-old silicate-activated GBS (pores ranging from ~2 to 10 nm in size, paste synthesised using 7 wt. % Na_2O relative to GBS in the form of Na_2SiO_3) using a water-to-GBS ratio of 0.5 (water-to-solid ratio of 0.47 taking into account SiO_2 in solution) [105]. Due to the lack of soluble silica in the activator, hydroxide-activated GBS (with a water-to-cement ratio of 0.5 and 7 wt. % Na_2O relative to GBS) consists of larger pores that are ~40 nm in size [105].

For systems based on N-A-S(-H) gels, such as alkali-activated FA (AAFA) and AAMK, the water-to-solid ratio and availability of aqueous silica from the activator has a large influence on the resulting pore structure. For AAFA synthesised using sodium silicate (3 wt. % Na_2O relative to FA in the form of Na_2SiO_3) and a water-to-solid ratio of ~0.34 the connected pore structure consisted of a bimodal distribution of pores at ~7 and 300 nm in size after 28 days of curing (at 40 °C) [106], while at the same sample age the pores in AAMK synthesised using sodium silicate (28 wt. % Na_2O relative to metakaolin in the form of Na_2SiO_3) and a water-to-solid ratio of 0.71 are ~25 nm in size (sample cured at ambient temperature, unpublished N_2 and MIP data similar to data reported in ref. [107]). The higher activator concentration used for metakaolin (Na_2SiO_3 activator with Na_2O concentration equivalent to 10M NaOH, [107]) compared to FA (Na_2SiO_3 activator [106] with Na_2O concentration equivalent to ~2M NaOH) and associated availability of free silica will likely have promoted more extensive dissolution of the precursor and amount of gel precipitated, leading to a more refined pore structure, although there is no direct evidence in the literature on this behaviour. However, when metakaolin is activated using a hydroxide-based activator (28 wt. % Na_2O relative to metakaolin with a water-to-solid ratio of 0.9) a very open connected pore structure evolves, consisting of pores that are ~100 nm in size after 1 year of curing (at ambient temperature, unpublished MIP data similar to data reported in ref. [107]).

These data show that a more refined pore structure for the connected network can be found in the Ca-rich cement systems (i.e., small pores making up the connected pore network), in good agreement with results from earlier research [108]. Furthermore, unless a very high alkali concentration is used along with an extensive amount of soluble silica (as is the case for sodium silicate-activated metakaolin), the connected pore structure of Ca-poor systems tends to consist of relatively large pores. The implications of these differences in pore structure on durability will be discussed below. It is important to keep in mind that, although closed pores may exist in cement paste that are relatively large compared with the connected pores (i.e., micron sized pores and air bubbles versus nanosized pores) [106], these larger pores are not involved in the transport of aggressive chemicals through the material [109], and therefore are a secondary consideration for the assessment of durability controlled by mass-transport processes. Moreover, it is the size of the pore entries/exits (throats) that controls diffusion of chemicals through the pore structure rather than the

size of the pore interiors [110]. Hence, although the ink-bottle effect in cementitious materials is known to artificially skew MIP results towards smaller pores (since larger pores exist but are not accessible at lower pressures due to the existence of constricted pore throats (i.e., pore entries/exits)) [111], information on permeability can be inferred from MIP-derived pore size distributions since this technique is sensitive to the pore throats that make up the percolating pore network. Therefore, to assess the size of pores controlling permeability of the paste, techniques that are sensitive to the pore throats are needed, such as N_2 desorption for pastes with pores less than ~50 nm in size [105] and mercury intrusion porosimetry for pores that are larger than those accessible using N_2 sorption.

Considerations for Alkali-Containing Binders

The development and implementation of low-CO_2 cements in industry require an in depth understanding of material performance across length and time scales. As outlined above, there are a range of material attributes that we now understand at a fundamental level that enables us to tailor the chemistry and physical properties of the product to obtain superior in-field performance. Specifically, discussion of the effects of Ca content, alkalis, and Al reveals that there is a complex interplay between these elements in alkali-containing cement systems that controls the stability of the binder phase and the attributes of the percolated pore network (including systems that contain some PC).

Importance of Calcium

It is clear that Ca is needed to obtain a low permeability material, which is attributed to water molecules strongly solvating Ca ions in contrast to the weaker solvation of Na ions, leading to structural and bound water being incorporated in the Ca-rich binder phase (i.e., C-S-H-type gel). However, additional analysis is required to determine the lower bound for the Ca content, below which permeability is adversely affected. Moreover, the effect of free silica in the alkali activator on the permeability is also apparent from the existing literature [112,105,109], and more research is needed to ascertain how silica, or other soluble species in the activator, contribute to the development of a low permeability pore network.

Balancing of Alkalis and Aluminium

Contrary to the historical avoidance of alkalis such as Na in PC concrete due to ASR, it is clear that a certain amount of Na can be present in a concrete mix based on alkali-activation, provided it is largely incorporated into the binder phase (C-S-H-type gel phase in Ca-rich systems). This has been known from a practical viewpoint due to the strong evidence of durable concrete structures that were made using sodium carbonate-activated GBS in the former Soviet Union [113] and Belgium [114]. However, now there is emerging scientific evidence based on atomistic simulations and experimental characterisation of phase-pure synthetic C-S-H-type gels [115,72,88,89]. Recent findings point toward the Na existing in the interlayer region of the C-S-H-type gel [72], which, unless accompanied by Al, is found to negatively augment the nanostructure of phase via the creation of a highly depolymerised gel [116]. Therefore, it is crucial that available Al is present in the Ca-rich AAM system during the early stages of reaction, since the Al is found to offset the depolymerisation effects of Na by increasing the MCL of the C-(N)-A-S-H gel [73]. The rate of Al release needs to be carefully controlled to avoid detrimental gel precipitates forming on the surface of reacting particles that significantly reduce the longer-term dissolution kinetics and subsequent gel formation [90]. There appears to be an upper limit of alkali incorporation into the C-S-H-type gel, beyond which the resulting structure is less stable (as found from quantum chemical calculations), even in the absence of a change in degree of polymerisation [88]. Although the alkalis are often

needed to kick start the reactions (i.e., dissolution and subsequent precipitation), overdosing must be avoided since it can lead to serious long-term problems.

Reaction Mechanisms and Kinetics

While we have a satisfactory understanding of the thermodynamics of cementitious phase formation [117], insight into the kinetics of hydration reactions for both blended PC and AAM systems is still lacking. Finely ground mineral powders are known to accelerate cement hydration rates. This 'filler effect' has been attributed partly to dilution when the cement content is reduced, and partly to the provision of additional surface area, which may provide additional sites for nucleation of the hydration products, hence accelerating reactions. Skibsted and Snellings [10] explain that kinetic barriers like water availability and pore space for hydrates to precipitate may constrain SCMs to reach full reaction, besides thermodynamic equilibrium considerations.

It is well known that the amorphous nature of SCMs will have a substantial effect on the rate of reaction and the extent of hydration to form binding phases. The role of Ca and alkali metals as a breaker of aluminosilicate networks is well understood, although it is not appreciated that some phases in FA with similar composition may be either glassy and reactive, or pseudo-crystalline and unreactive [118]. High cooling rates have a generally positive effect on slag reactivity, as it can be linked to either a high glassy phase content or to preservation of more reactive high-temperature crystalline phases such as β-C_2S instead of γ-C_2S, as demonstrated for different types of steel and other slags [10]. Partial crystallisation or unmixing of two compositionally different glasses may occur when cooling rates close to the critical cooling rate are used (i.e., the minimum cooling rate to obtain an entirely vitrified solid). As shown by [119] for the re-smelting of basalt, controlled phase separation may lead to increased reactivity of the glass by removal of constituents that render the glass less soluble, such as Fe_2O_3, MgO or TiO_2.

As postulated by Skibsted and Snellings [10], the dissolution of a glassy phase in SCM results in a 'modified layer' rich in Si formed by the release of Ca ions and hydrolysed Al units. Hydrated Ca ions and aluminate species will re-adsorb on the modified layer via cation-exchange or electrostatic interactions. By using a micro-reactor, Suraneni et al. [120] observed that the presence of Ca and Al in solution strongly inhibits dissolution of GBS. It is generally accepted that dissolution of SCM is initially the rate-limiting step in binding phase formation in blended PC. However, there remains uncertainty about the rate-limiting step at later ages. Scrivener et al. [121] made a convincing case that the rate-limiting step in the later hydration of alite is neither dissolution nor diffusion through product layers, but instead the rate of growth of C-S-H needles and thermodynamics (e.g., solubility, degree of (super)saturation). The prospect that the interplay between nucleation and pore solution composition, rather than dissolution, controls hydration kinetics in high SCM-PC blends and AAM requires investigation.

It has been demonstrated that nanoparticle seeds added to AAM eliminate the induction period by catalysing the formation of nuclei, which in turn, enhances dissolution of the precursors [122,123]. While the filler effect in PC blends has been assumed to provide nucleation sites for C-S-H, Berodier and Scrivener [124] showed that it pertains only to limestone. Other SCMs acting as fillers do not enhance nucleation meaningfully, but instead reduce the interparticle distance and increase the shearing, which promotes nucleation. Surface charge and adsorption of Ca and silicate species onto the filler surface play a key role in the effectiveness of nucleation [125], which explains why limestone is an effective filler for PC blends. There remains much scope to clarify the mechanisms of the filler effect and nucleation in AAM and PC blends with high SCM content. Bellman and Stark [126] showed that GBS can be activated by Ca salts together with a small amount of limestone, PC and/or lime. They ascribe the enhanced activity of the GBS to the lower pH and the concomitantly higher Ca concentration in the pore solution, caused by the Ca salts. The question

must be asked to what extent nucleation and surface charges played a pivotal role in the success of this activation system. Monkman et al. [127] showed that the injection of captured CO_2 into concrete accelerated hydration through the formation of nano calcite as nucleation sites. It will be interesting to see how injection of CO_2 impacts on AAM and PC blends with high SCM content.

Surface Chemistry and Plasticising Admixtures

Extensive research has been published on reaction mechanisms in blended PC and AAM systems. In contrast, there is a sparsity of literature on surface chemistry related to either blended PC or AAM, resulting from the complexity of designing experiments simulating the pore-gel-solid interface in reacting cementitious systems. Moreover, surface chemistry studies usually focus on either blended PC or AAM, and unfortunately do not view these cements as a continuum. This binary approach has resulted in a gap in our understanding of how a change in pore solution affects the surface charges on various cementitious precursors and binding phases. Consequently, there has been inadequate development of admixtures, especially plasticisers, for systems involving a combination of, or a shift between, positively and negatively charged particles. Disappointingly, comprehensive reviews on admixtures in cement [128-130] have under-emphasised the importance of surface chemistry in designing the architecture of plasticising polymers.

Skibsted and Snellings [10] explain that dissolution of a glass (from FA or GBS) is slow at near neutral pH, giving a modified layer rich in Si formed by the release of Ca^{2+} ions and hydrolysed Al units. Hydrated Ca^{2+} ions will re-adsorb on the modified layer via cation-exchange reactions or electrostatic interactions between the negative surface and the positive ions. Dissolution is enhanced significantly at higher pH with network hydrolysis and ion-exchange processes taking place at the same time, providing an increased release of silicate species. Deprotonation of the hydrated Ca^{2+} ions at high pH results in stronger interaction with the hydrolysed silicate and aluminate species, which may lead to condensation reactions that may form a passivating layer of low Ca/Si C-A-S-H.

While the surfaces of oxide minerals are normally negatively charged at high pH, the balance between anions like OH^-, CO_3^{2-}, Cl^-, and SO_4^{2-} on the one hand, and cations like Ca^{2+}, Mg^{2+}, Na^+, and K^+ on the other hand, may determine the net charge, hence zeta potential [131-133]. In PC blends the dominance of Ca^{2+} will cause a positive charge reversal on most precursor surfaces, including alite, belite, limestone, calcined clay, GBS, and FA, as well as C-A-S-H binding phases, but not on quartz or silica fume, which remain negatively charged [131,132]. A higher aluminate content in the precursors gives a more positive zeta potential, while a higher silica content gives more negative zeta potential [133]. Expectedly, Ersoy et al. [132] observed that carbonation causes more negative zeta potential owing to the removal of adsorbed Ca^{2+}. While Ca^{2+} and Cl^- ions affect zeta potential greatly, Na^+ does not appear to have an effect on PC-slag cement [133], probably because Na^+ is mobile and more soluble than Ca^{2+}, which preferentially adsorbs onto negatively charged surfaces instead of Na^+.

This observation has implications for AAM, where the surfaces are strongly negatively charged instead of blended PC cements with positively charged surfaces [134]. However, Kashani et al. [135] showed that the dependence of zeta potential on pH, the type of alkali cation and the soluble silicate concentration is more complex than appeared from other studies. It was shown that the addition of NaOH or KOH to a suspension of slag caused a transition from negative to positive zeta potential, which increased with higher dosages of the hydroxide activators, and was in contrast with the expectation that the silanol groups would become more extensively deprotonated at high pH, yielding a negatively charged surface. Clearly, the release of Ca^{2+} from the slag through partial dissolution and interaction with dissolved alkali cations led to a significant effect on surface chemistry, with a higher positive zeta potential observed for KOH than NaOH. Conversely, addition of sodium metasilicate to slag caused higher negative zeta potential as silica was adsorbed.

Most research on and commercial development of plasticising polymers have focused on PC blends, assuming that most of the particle surfaces are positively charged. Therefore, anionic polymers like polycarboxylate ethers (PCE) have been developed to attach to the Ca^{2+} dominant positively charged surfaces and cause steric hindrance, hence dispersion. Liu et al. [130] used density functional theory (DFT) to show that the binding strength of Ca^{2+} with superplasticiser groups decreased in the order, phosphonate > phosphate > carboxylate > sulphonate > sulphate > alkoxide. Much work has been done to tailor the architecture of the plasticiser to the characteristics of precursors. For example, Khayat et al. [136] explained that two different PCEs are required for PC-silica fume blends to give preferential adsorption onto each precursor. Plank et al. [128] stated that blended cements with low PC content require polymers with a high ratio of side chains. In blended PC with high FA content, Ng and Justness [137] observed that the plasticiser interacted more with PC than with FA. While the improved rheology of ternary PC-slag-FA blends can be ascribed partially to the use of PCEs, Kashani et al. [138] demonstrated that a widening of the particle size distribution plays a pivotal role.

Stecher and Plank [139] developed one of the few available phosphate comb polymers (instead of PCE) for low water/binder, which is relevant to low-CO_2 emissions concrete. A substantial maldistribution of charge density between precursors, or an excessively positive charge on a precursor like calcium aluminate cement (CAC) may render a PCE ineffective. Akhlaghi et al. [140] used phosphonic groups to lower the adsorption affinity of PCEs to the surface of CAC particles, hence restraining the change of surface potential upon adsorption. The same principle may be utilised in the development of plasticisers for similar low-CO_2 cements.

When NaOH with low sodium silicate addition was used to activate a FA-slag concrete, Keulen et al. [141] showed that an anionic PCE can give effective plasticising, which confirms the zeta potential observations by Kashani et al. [135]. Similarly, Marchon et al. [142] demonstrated the effectiveness of a PCE to plasticise an NaOH activated PC-FA blend (hybrid cement). While Conte and Plank [143] managed to plasticise an NaOH-activated slag using a PCE, they did not succeed when activating the slag with sodium carbonate. In alkali-activation of FA-slag concrete with higher silicate addition, giving negatively charged surfaces, anionic PCEs do not give convincing results [144]. Likewise, Liu et al. [145] obtained unsatisfactory results when using a cationic surfactant to disperse a high silicate activated system. Kashani et al. [138] demonstrated that cationic polymers with long side chains gave enhanced yield stress reduction compared with the anionic equivalent in AAGBS. Although most cationic polymers have been developed for adsorption onto clay surfaces at lower pH [146], there is an opportunity to develop cationic copolymers for plasticising AAM with higher silicate addition.

For this purpose, Kraus et al. [134] developed a class of cationic copolymers where the cationic charge is due to the presence of certain cyclic and/or polycationic groups that are stable towards Hoffmann elimination that would otherwise occur at very high pH, leading to a decay in positive charge over time and a loss of slump retention. Moreover, the high pH that is required for activation also constitutes a high ionic strength, which may eliminate the dispersion effect that is possible at lower pH. Although developed for plasticising gypsum, the cationic comb polymer developed by Hampel et al. [147] may inspire further work in alkali-activation. The demonstration by Jiang et al. [148] that amphoteric polycarboxylate polymers give superior performance to anionic PCEs provides a useful reference to researchers tailoring plasticiser architecture to suit lower pH AAM or blended PC cements where there may be positively and negatively charged particles present at the same time.

Unfortunately, only anionic PCE plasticisers are available commercially at present. The type of cationic copolymers described by Kraus et al. [134] and amphoteric polymers that are stable in high

silicate AAM are not available commercially. This obvious gap in plasticiser development is a key obstacle in the commercial adoption of AAM. Moreover, most published work on alkali-activation has used poorly plasticised conditions. Therefore, it is not known yet how the microstructure and hence durability will change when an effective plasticiser is used in alkali-activation. The micro-cracking often observed in AAM can potentially be reduced when a lower dosage of silicate and lower water/binder ratio are used.

Electrically-Enhanced Supersonic Shockwave Reactors

PC clinker and GBS granules are usually ground in large, vertical roller mills that are capital intensive and located in association with PC operations. It is not practical to use such equipment in smaller markets or in a geographically distributed manner to exploit smaller waste streams such as metallurgical or steel slag, or virgin materials like volcanic ash or rock. This limitation on grinding practice has consolidated the position of large cement companies in smaller and remote markets, even when local material could be used as SCM. Loesche [149] in Germany has recognised this limitation and now has a compact vertical roller mill available for remote locations where a customer will grind PC clinker and/or GBS granules in smaller volumes. IMPTEC in South Australia has developed an innovative gyratory crusher with excellent capability for comminution of cementitious materials [150]. Universal Vortex in Melbourne, Australia, has developed an acoustic grinder that produces a shock wave generated in a precisely designed geometry to shatter brittle materials, which has been demonstrated at scale for PC clinker and GBS granules [151]. The advantage of the Universal Vortex is that it fits into a shipping container, so it is mobile and can be deployed easily in remote locations for the grinding of local material.

The electrically-enhanced supersonic shockwave reactor (EESS) invented by Lansell et al. [152] is a further advance in the intensified processing of materials. It is common knowledge that rocks and minerals have a high compressive strength but relatively low tensile strength, which is the rationale behind the use of steel to reinforce concrete. Most comminution devices use compressive forces and to a lesser extent shear forces to fracture particles, because it is not straightforward to place a particle in a tensile field. It is not common knowledge that an electric field substantially reduces the tensile strength of a particle. The invention by Lansell et al. [152] subjects particles to a tensile stress within an electric field, which requires ultra-low energy of fracture. This concept uses high current and is different from the high voltage pulsing system developed by Andres [153], which also subjects particles to tensile fracture.

Besides comminution, the EESS can also be used for high-intensity chemical reactions, including decarbonising of limestone, calcination of clay, formation of PC, smelting and rapid cooling of glasses, metallurgical reduction of ores, and gasification of waste. For chemical reactions to proceed, the change in Gibbs free energy needs to be negative, which is usually achieved by increasing the temperature, for example to 1,450 ºC in a cement kiln. The problem with a high temperature is that materials of construction become a limiting factor in reactor design and the choice of chemical processes. In contrast, when an electrical field is used, a lower temperature rise can be achieved, which has huge potential in reactor design. Little has been published on this new field of science, besides De Knoop et al. [154] that showed how the electrical field in a TEM can melt gold at ambient temperature by transforming a perfectly crystalline phase into a disordered phase. The engineering of such a system at scale is not straightforward, but several options are feasible to extend the technology proposed by Lansell et al. [152]. Figure 5 depicts such a system operating at pilot scale of 10 tonne per hour, converting waste to synthesis gas.

Figure 5. An electrically-enhanced shockwave reactor of 10 tonne per hour without feeding system fits into a 20 ft container. Here, the reactor is configured to gasify solid waste for energy generation.

The EESS is a highly efficient comminution device and at the same time a chemical reactor, so it is possible to transform virgin and secondary materials both physically and chemically in a way not possible with existing technologies. By varying pressure, current and frequency, it is possible to control particle size of the product. Moreover, it is possible to rapidly cool products and hence preserve the glassy state (if required) using a venturi system. Compared with cement clinker production in a rotary kiln, the EESS dictates a simpler and more compact plant design, because operating temperatures are lower and hence there is less need for heat recuperation. Moreover, there is no need for fine-grinding of raw meal ahead of clinker production, as the EESS provides an intense mixing environment where crushed feed materials are rapidly reduced in size and homogenised. Equally, there is no need for a clinker grinding mill, as the product from the EESS is already at the required particle size. An alternative processing technology for the calcination of clay is the flash calciner which has been well proven at production scale [155], although it can be expected that the EESS system is likely more compact and mobile. Microwave processing of cement clinker [156]has been proposed in an attempt to lower the reaction temperature, but again, longer reaction times are expected than in the EESS.

The application of EESS raises several questions about cementitious reactions that cannot be answered from our existing knowledge base and require further research. For example, alite and belite are the main reactive phases formed by the clinkerisation process in rotary kilns. It is known that the temperature in the kiln must be sufficiently high to form alite. If the cooling rate is too slow, less reactive phases may stabilise. However, what has not been contemplated is the high cooling rate in EESS that may create and then freeze a glassy phase rather than alite and reactive belite polymorphs. It is likely that a frozen glassy phase is more reactive than conventional clinker phases. However, it is not yet known to what extent there may be micro crystalline inclusions in such a glassy matrix. Moreover, the relationship between clinker or cementitious microstructure and dissolution rate is poorly understood, so further research on EESS produced phases will deepen our insight into cement science.

Selection of New Source Materials

Historically, industry and academia have been interested in substituting PC clinker with alternative materials (SCMs) that provide comparable or higher performance at lower cost and environmental impact. Presently, there is an increasing interest in use of lower quality primary resources as well as secondary resources as substitute materials (aligning with increasing interest in perspectives like the circular economy and environmental protection). This substitution strategy is generally considered

to be economically and environmentally beneficial, and readily implementable, since its basis is PC production technology. Such primary resources include clays with lower purity than industrial clays [16,157]. Secondary resources may include industrial by-products, including slags from metal ore beneficiation processes [158,159], as well as post-consumer wastes such as ashes from incinerators [160,161]. Since these resources have different chemistry to conventional raw materials for PC production, high substitution rates of these resources for PC clinker can significantly modify solid phase stabilities in the resulting binders. This presents its own challenge and research need – to predict properties of highly substituted PC binders. However, for this substitution strategy to be applicable at the massive of global cement production, which is needed to realise its potential benefit as a climate change mitigation measure (i.e., to reduce CO_2 emissions), sufficiently high availability of substitute resources is required [162]. This is typically not an issue for primary resources like clays, which are globally abundant, but is potentially problematic for secondary resources.

Secondary resources are inherently supply limited and have varied quality, due to their nature as by-products of industrial processes and public consumption. This limits their practical applicability as single PC clinker substitutes at the mass (i.e., global) scale, especially due to their local variability (in amount and quality). However, their feasibility as PC clinker substitutes may be somewhat improved by simultaneous use of multiple secondary resources as a substitute mixture; the chemistry of such a substitute mixture may be controlled by homogenisation processes analogous to those commonly employed in preparation of PC clinker feed. Such an approach has been little explored to date, yet may be feasible at a significantly larger scale than single resource substitution (but not necessarily at the same scale as PC production), especially when coupled with thermodynamic modelling to guide homogenisation processes towards use of substitute mixtures that result in high performance cementitious binders. It is likely that this will require thermodynamic data and models to be developed for solid phases and aqueous components not currently specified in thermodynamic databases for cement systems. Enabling this approach will require determinations of reactivities of (primary and secondary) resources under appropriate curing conditions to reliably provide time dependent material property insight (i.e., during cement hydration) [163].

These substitution strategies can be more comprehensively employed at the clinker production process; specifically, to substitute conventional raw materials fed into this process. Here, use of thermodynamic modelling to guide solid phase formation under clinker production processing conditions is desirable. The availability of reliable thermodynamic models for potentially stable solid phases at such conditions, i.e., high temperature, is arguably poorer than at conditions experienced during cement hydration, including for PC systems. Development of such thermodynamic models for use in alternative clinker systems, e.g., ye'elimite for the calcium sulphoaluminate system [164], especially for materials with more novel chemistry, will be key to unlocking their potential. These thermodynamic models will also facilitate the development of non-traditional processes for clinker production, e.g., electrification and utilisation of concentrated solar power, since thermodynamics provides a fundamental and general basis to understand chemical reactions and their driving forces. This research is also needed to systematically understand how construction and demolition waste concrete can be processed into reactive cementitious material in an economically and environmentally beneficial manner, for which the potential is undoubtedly massive.

Thermodynamic data need to be collected for the type of glassy and crystalline phases that can be formed in the EESS system described above. Secondary product sources such as waste clay, metallurgical slags, unreactive FA, coal tailings, and sewage biosolids that cannot be used as SCMs at present could be processed in pre-determined combinations in the EESS to produce cementitious phases that may be hydraulic on their own, may be alkali-activated, or used as SCM in PC blends.

These secondary product sources may be supplemented by virgin materials like basalt, volcanic ash, and oil shale ash. The application of EESS or similar technologies will unlock new source materials and create a new value chain for cementitious materials, often in a geographically distributed manner, provided that the obstacles of restrictive standards can be overcome, as discussed below.

Scrivener et al. [16] state that secondary products like FA and GBS are in short supply, but that clay waste and limestone are in abundance, which provides the rationale for LC^3 cements. The Earth's crust is composed of approximately 61% SiO_2, 16% Al_2O_3, 7% Fe_2O_3, 6% CaO, 5% MgO, 3% Na_2O and 2% K_2O. Figure 6 depicting the composition of several virgin materials and secondary products reflects the limitation that most SCMs and potential SCMs are Al-Si-rich and Ca-poor. As stated before, it is essential to have sufficient Ca in C-S-H, which means that there is a strategic need to identify alternative sources of Ca to supplement other source materials when subjected to cement-forming processes like EESS. As shown in Figure 6, biosolids ash (30-50% of biosolids) has a high percentage of Ca and could be converted to cementitious material, with the organic content of the biosolids being converted to fuel using electrically-enhanced supercritical conversion. Basalt has a reasonable Ca content and could form a suitable precursor, provided it is in a glassy state [165]. Some volcanic ashes also have a higher Ca content and may supplement the Ca deficiency in clays during cement or precursor synthesis. There is an abundance of shallow oil shale in several countries, but they are not economically viable using existing technology. By combining electrically-enhanced supercritical conversion with a process like EESS, it is possible to convert the organic content into fuels and at the same synthesise cementitious materials utilising the high Ca content of oil shale (Figure 6). New sources of Ca-rich secondary products will facilitate the wider utilisation of Ca-poor secondary sources like waste clay and FA with low reactivity.

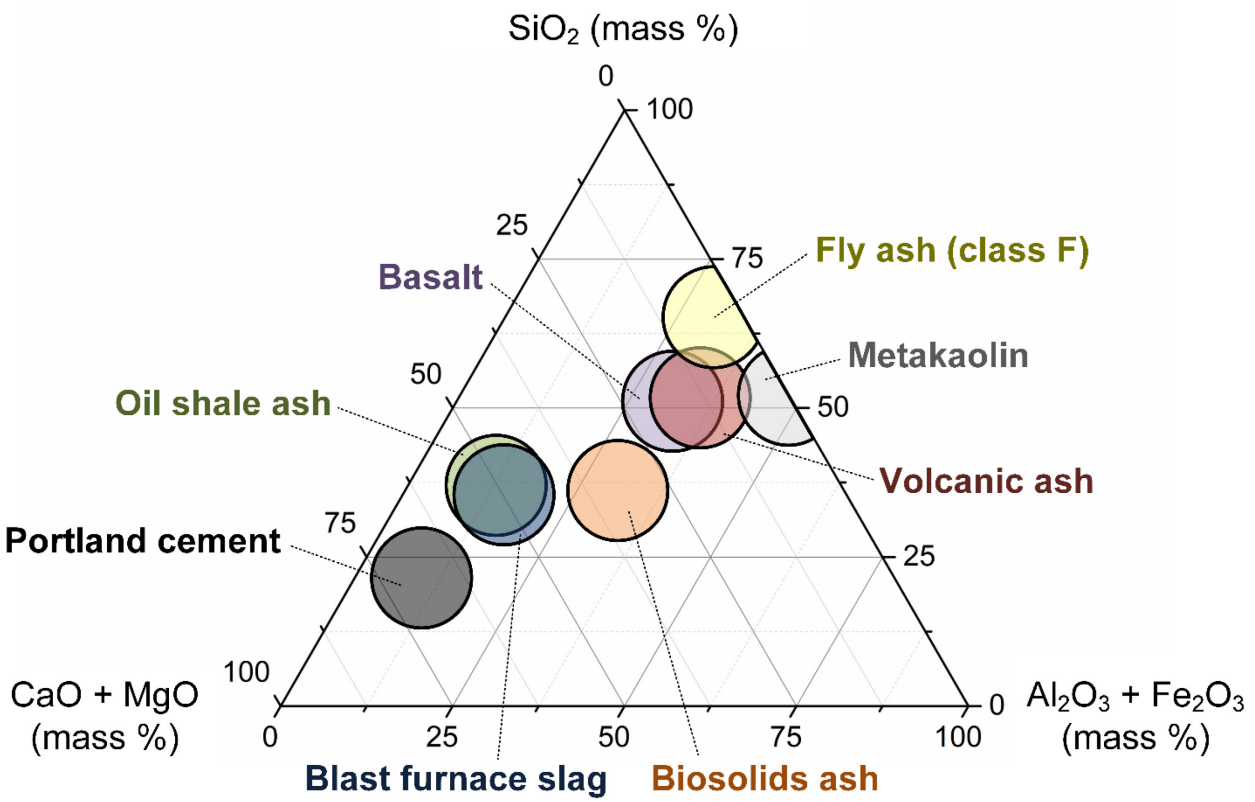

Figure 6. Phase diagram showing the composition range of various virgin and secondary cementitious source materials

Ke et al. [166] showed that the addition of a calcined hydrotalcite to a sodium carbonate-activated GBS enhances carbonation resistance. Bernal et al. [167] demonstrated that the hydrotalcite formed

in-situ from the alkali-activation of a GBS with high MgO content has similarly high carbonation resistance. It appears that if MgO is present as a silicate in a glassy GBS, it has a beneficial effect on the durability of the cement binder. In contrast, the MgO content in limestone is usually restricted to 5 wt.%, because MgO tends to remain as high smelting periclase in clinker that slows down hydration and causes delayed expansion. If the EESS can integrate MgO in impure limestone or secondary materials into the glassy phase, it may expand the range of cementitious source materials to include dolomitic limestone, and also enhance the performance of the resulting concrete. This area offers a substantial opportunity for research and commercial development.

The focus of this paper is cementitious binders and how they impact concrete properties, rather than secondary materials such as waste glass and recycled concrete that can be used as aggregates and sand to reduce the CO_2 footprint of the concrete. The recycling of construction rubble is receiving increasing attention in the literature and in industrial practice [3,6]. What has not been considered widely is the selective recovery of harder unhydrated cement particles from the softer hydrated cement particles attached to the larger sand and aggregate particles in recycled concrete. In some concrete almost 50% of the cement particles remain unhydrated and could be reused without an additional CO_2 penalty. In conventional crushing of recycled concrete, these unhydrated cement particles become contaminated by fines from the comminution of sand and aggregate. Smart Crusher BV in the Netherlands developed a crushing system that can recover selectively the unhydrated cement without reducing the size of the sand and aggregate. It is evident that innovation in processing equipment can contribute substantially to the expansion of the cementitious material supply chain.

Durability Considerations

Mindess [168] gives a broad overview of the factors affecting the durability of concrete structures, where Figure 7 depicts conceptually the mechanisms governing the durability of reinforced concrete. The chemistry of deterioration of AAM is different [169] to that of PC blends, but the same factors still need to be considered. Briefly, the durability of a concrete composite is a function of (a) the chemical stability of the binding phases and residual precursors when exposed to aggressive agents, including atmospheric CO_2, (b) the expansive and destructive nature of undesirable phases that form over time, (c) cracking resulting from physical and/or chemical stresses, (d) permeability of the matrix, and (e) corrosion of the steel reinforcement. Concrete durability is a complex subject, so only selected observations are made here with the aim to identify new research opportunities and how durability impacts on commercial adoption.

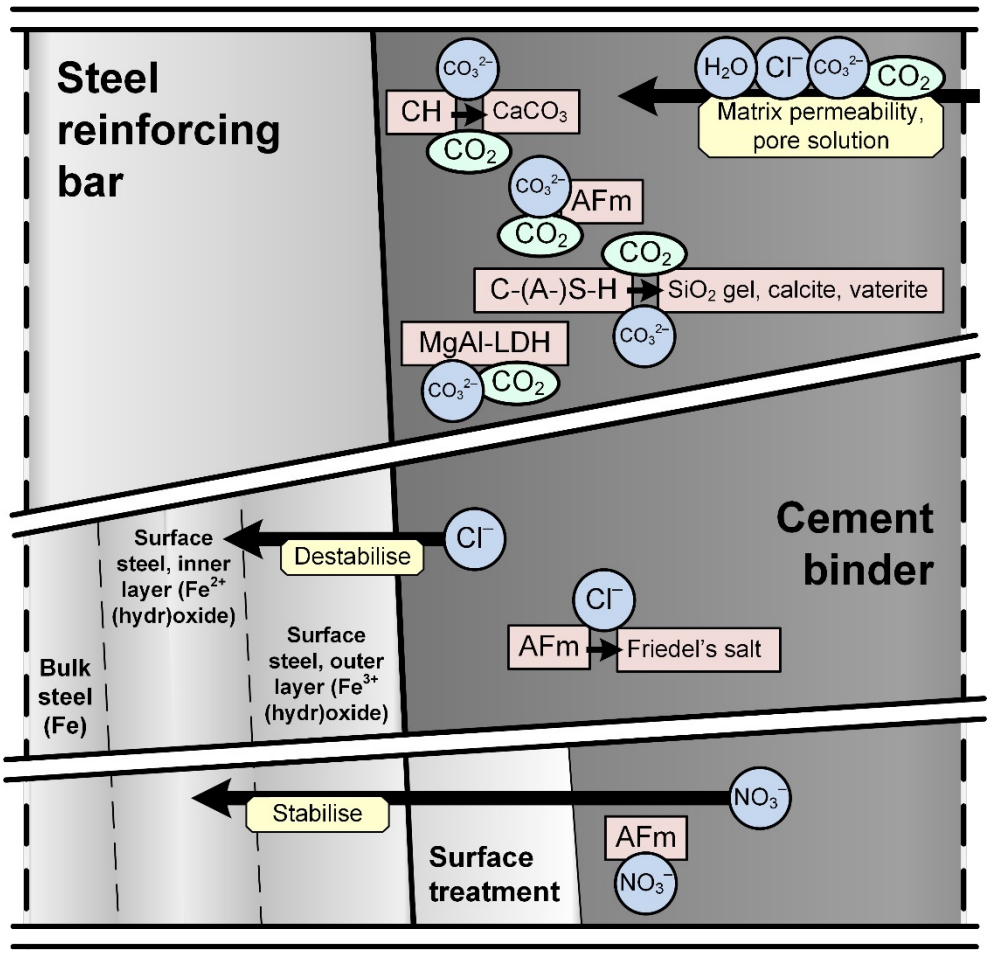

Figure 7. Conceptual diagram of the mechanisms and factors affecting the durability of steel-reinforced concrete

Pore Structure

The pore structure of cement paste and associated permeability is known to control the rate of ingress of aggressive chemicals such as CO_2, sulfates and chlorides [170] (referred to as *matrix permeability* in Figure 7). Hence, being able to elucidate and manipulate this property for PC blends and AAM is an important step toward moving these materials from laboratory research to industry. There are a number of techniques capable of measuring the permeability of cementitious materials, including beam-bending, dynamic pressurisation, thermopermeametry, and the application of high-pressure [104]. For PC, the permeability begins at ~0.01 nm^2 7 days after curing (for w/c ratio of 0.5) and decreases to between 0.001 and 0.01 nm^2 as curing progresses [104]. For the AAGBS discussed above, the permeability of silicate-activated GBS 7 days after curing is 0.0001 nm^2, while for hydroxide-activated GBS at the same age it is ~0.1-0.5 nm^2 [105]. Hence, there is the possibility of manipulating the activator chemistry for Ca-rich AAM such that a desirable permeability value is obtained. Ca-poor AAM tends to be on the higher side for permeability, where silicate-activated class F FA (outlined above) has a permeability of ~0.1 nm^2 at 7 days of 40 °C curing [109], while silicate-activated metakaolin (28 wt. % Na_2O relative to metakaolin in the form of Na_2SiO_3) has a permeability of ~0.4 nm^2 at 5 days of curing (unpublished beam-bending data). These more permeable systems will allow for quicker migration of aggressive chemicals through the connected pore network, and ultimately to the site of steel reinforcement if present.

From the data reported above, it appears that Ca is a crucial constituent for obtaining a refined pore structure and associated low permeability. However, for AAM this alone does not necessarily lead to a low permeability. It is also clear that free silica has a profound impact on the permeability,

which cannot be solely attributed to the overall water-to-solid ratio (see silicate- and hydroxide-activated GBS data outlined above, water-to-solid ratios of 0.47 and 0.5 respectively) [105]. Different activators are known to have distinct effects on the temporal evolution of the extent of reaction [91,171,172], and the type, amount and location of gel that has precipitated [173-175], which, in turn will affect the connect pore structure and associated permeability.

Pore Solution Chemistry

Historically, protection of steel reinforcement in concrete has involved two mechanisms: (i) low permeability of the cement matrix and (ii) pH buffering from solid portlandite [176]. Steel will not corrode when exposed to the high pH pore solution of PC (pH ~13), and therefore as long as solid portlandite is present in the concrete the pH drop associated with the acidifying effects of CO_2 (and magnesium sulphate) is avoided. However, as industry moves toward more sustainable cement options it is important that the topic of steel passivation is revisited. Blended PC often relies on portlandite and the associated pozzolanic reaction, which provides additional C-S-H-type gel formation and associated strength and pore structure development [177]. However, there is a limited supply of portlandite in hydrated PC, and as industry pushes the limit on clinker replacement the amount of portlandite in concrete is likely to approach zero. For example, a 30% replacement of white PC with metakaolin or metakaolin and limestone leads to less than 10% of the amount of portlandite being present compared with a neat white PC at 91 days [178]. This residual amount of portlandite will therefore have 10% of the buffering capacity as compared with a neat PC. Pushing the limit on clinker substitution beyond a 30% replacement is likely to result in minimal pH buffering capacity. Nevertheless, if this loss of portlandite is offset by the creation of a more refined pore structure and associated lower permeability, then the overall durability of the system will be maintained. Studies on these systems show that this is indeed the case, where white PC (w/c ratio of 0.4) consisted of pores ~10-20 nm in size at 91 day while the blended counterpart (30% replacement with metakaolin or metakaolin and limestone) had pores ~7-10 nm [178].

For non-PC systems, such as AAM, the lack of a pore solution buffer has often been cited as a reason why these systems will have lower durability. However, similar arguments to those on blended PC can be used to show that even without a solid buffering phase, the overall durability of the material can be comparable to neat PC. Moreover, alkali-containing systems (i.e., those containing Na or K) have a significant concentration of alkalis (i.e., Na) in the pore solution [179-182]. This high concentration is similar to NaOH solutions that are effective at CO_2 capture (other systems known to be effective at CO_2 capture include amines), and such high alkali solutions are known to have a high capacity for CO_2. Hence, the pore solutions of AAM should also have a high capacity for CO_2 as quantified below. The amount of CO_2 that can be absorbed by a saturated calcium hydroxide solution is ~0.05 M [183], and this absorption will lead to a drop in pH from 13 (as measured experimentally by Han et al. [183]) to 9.4. For a 1 M NaOH solution (pH of 14) the amount of CO_2 that can be absorbed is ~0.85 M [184], which is much higher than the CO_2 capacity of saturation calcium hydroxide solution. Furthermore, the absorption of this amount of CO_2 will lead to a pH drop to 9.2, on par with the final pH of the calcium hydroxide solution. It is important to note that the effects of phase solubility have not been taken into account in this calculation (i.e., potential dissolution of C-S-H-based and N-A-S(-H) phases along with secondary phases), nor has the potential precipitation of solid sodium carbonate and calcium carbonate phases, both of which are required to obtain more accurate values for the final pH levels. Nevertheless, it is clear from the data reported above that alkali (i.e., NaOH) pore solutions have a much higher CO_2 capacity, which implies that AAM will be more resistant to a detrimental drop in pH compared with blended PC when exposed to the same CO_2 conditions, and with comparable pore structures, the alkali-containing cements will be more resistant to CO_2 induced steel corrosion [185].

Combating Steel Corrosion

It has been explained before that LDHs like hydrotalcite (either as a mineral admixture or formed in-situ) absorb CO_2 entering the concrete, and hence reduce carbonation and steel corrosion (see Figure 7). It has been demonstrated that surface treatment of PC concrete by sodium silicate and sodium fluorosilicate decreased carbonation depth, as they react with PC [186]. Such surface treatment has not been investigated for AAM and PC with high SCM content. By using calcium stearate as an admixture, Li et al. [187] showed that the microcracking in AAGBS was eliminated and the pore structure was enhanced. It is not clear whether this improvement is a result of the action of the stearate, or whether the presence of a Ca salt is shifting the solution chemistry such that less Na is taken up in the C-A-S-H. Nevertheless, the calcium stearate can be expected to enhance carbonation resistance in AAM, although this still needs to be proven.

Balonis et al. [188] proposed the use of functional coatings consisting of CAC and calcium nitrate or nitrite in order to mitigate/delay initiation of steel corrosion in PC concrete (referred to as *surface treatment* in Figure 7). The principle is that AFm phases that form by reaction of the CAC will have a high capacity for both nitrate and Cl^- anions. The interlayer site occupation preference of AFm is as follows: $Cl^- > NO_3^- > NO_2^- > CO_3^{2-} > SO_4^{2-} > OH^-$. This highlights the competition for occupation of the AFm interlayer position amongst various anions e.g., Cl-AFm would form at expense of NO_3^--AFm or NO_2^--AFm if Cl^- mobile ions were present. Therefore, as Cl^- anions enter the concrete pore solution, they get absorbed into the AFm, which in turn releases nitrate or nitrite anions, which have been known to stabilise the ferrous oxyhydroxy inner layer protecting the steel.

In addition to the analysis of CO_2 absorption capacity of cement-based pore solutions, recent research has shown that sulphide associated with GBS can significantly reduce the susceptibility of steel to chloride-induced corrosion [189,190]. It is well known that Cl^- ions cause steel to undergo corrosion even in alkaline conditions (i.e., pH of 13) due to the ability of Cl^- ions to penetrate the passivating oxide layer and cause the release of Fe^{2+} ions from the metal [191], as shown in Figure 7. The main approach to combating Cl^--induced steel corrosion in PC is to use SCMs to obtain (i) a low permeability material and (ii) a high Cl^--binding capacity [191]. However, it has been shown recently that AAGBS concrete is highly resistant to Cl^- -induced steel corrosion [189,190]. Although the conventional test method used to assess steel corrosion resistance (i.e., redox potential) indicated that the pore solution chemistry of AAGBS is conducive for corrosion to occur, it was found that the embedded rebars in this system showed no evidence of pits or corrosion products, in contrast with the rebar embedded in the white PC system [189,190]. The high redox potential in the AAGBS system was attributed to the redox chemistry of aqueous sulphur (originating from GBS) and specifically oxidation of sulphide, while the surface of the steel was found to be rich in Fe-S species [189,190]. Hence, although the electrochemical findings point toward significant steel corrosion, it is clear that AAGBS concrete is highly resistant to Cl^--induced steel corrosion. Nevertheless, additional research is needed to uncover the underlying mechanism responsible for the enhanced corrosion resistance in AAGBS concrete.

It is evident that application of conventional wisdom from PCs often underestimates the performance of AAM, and more research is needed on such emerging materials to elucidate the underlying chemical and physical properties controlling macroscopic performance. This includes careful assessment of the performance and applicability of existing test methods, together with the need to redesign certain tests that are found to incorrectly categorise alternative cements, such as AAM, as inferior to standard PC. As explained by Li and Li [192], cracking can severely impact on concrete durability. The prediction of cracking and the healing of cracks in AAM and PC blends with high SCM are not well understood and require substantial research.

Basalt Fibre Composite Rebar Replacing Steel in Reinforced Concrete

It has been suggested that Roman cements with their proven exceptional durability should be used instead of blended PC in order to decrease CO_2 emissions [15]. The problem with this argument is that in the design of Roman-type cements there was no requirement to achieve low permeability as well as long-term residual alkalinity to protect steel reinforcement. Roman concrete was in compression as their dome and arch designs avoided tensions, hence utilised the high compressive strength of concrete in order to overcome its low tensile strength. In contrast, in modern structural design it is essential to use reinforcement material such as steel with high tensile strength in order to compensate for the low tensile strength and low modulus of elasticity of concrete. Therefore, the durability of reinforced concrete composite is determined largely by the ability of the cementitious binder to protect the steel against corrosion. Despite the general belief that a high pore solution pH is necessary for steel protection in blended PC, there is controversy about the role of pH in steel corrosion in unconventional cements. For example, Walling and Provis [193] suggested that magnesium phosphate cement, with its residual pH (of typically $6 < pH < 10$ [194]) is too low to protect against steel corrosion. On the other hand, Sharkawi et al. [195] showed that magnesium phosphate concrete provided superior protection of steel rebar in comparison with PC concrete. The uncertainty about the ability of new binders with low CO_2 emissions to protect steel against long-term corrosion is one of the main obstacles inhibiting their adoption. Moreover, the general belief that a high residual pore solution pH is required, even in the absence of steel reinforcement, limits the possible binder designs that may be acceptable to the construction industry.

Work has been in progress to replace steel rebar by carbon, glass or basalt fibre reinforced polymer (BFRP) rebar [196-198]. Although carbon and glass fibre reinforced polymer rebar has also been used in practice, there is more information available on the properties and CO_2 profile of basalt fibre, which is the focus of discussion here. Basalt fibre was first developed in Russia during the 1960s. Today basalt fibre and BFRP rebar are produced mainly in China and Russia, with basalt sourced from Ukraine. Apparently, there are only a few producers in Europe and one in the USA. Consequently, BFRP is largely unknown in the construction industry and substantial work is required before it may be adopted more widely, even for selected applications.

Basalt consists mainly of plagioclase, pyroxene and olivine, so the relative content of silica, alumina, lime, magnesium oxide, and ferric oxide determines the physical and chemical properties of the molten rock and the resultant fibres. Quality control of the basalt rock composition is key to the quality of the final BFRP rebar, which has been a problem with some suppliers. The basalt rock is smelt at 1400 to 1600°C and extruded into continuous filaments with a diameter of 12-18μm, which are glued together with an epoxy resin. The fraction of resin varies from 20 to 40 vol.% of the total BFRP rebar and varies between manufacturers. The BFRP rebar is then pre-stressed to up to 50% of its ultimate strength, prior to use as reinforcement in concrete. Antonopoulou et al. [199] explains how additional helical reinforcement and a braided configuration of the BFRP rebar can enhance its properties. Although there are no reports on the use of an inorganic binder such as magnesium phosphate [200] to replace epoxy resin in BFRP, the possibility deserves attention by researchers. Inman et al. [198] estimated that 87% of the CO_2 emissions of BFRP is attributable to the resin, which warrants the search for a binder with lower emissions.

BFRP rebar has a tensile strength in the order of 1000 to 1300 MPa, significantly higher than that of steel (500 MPa) [198]. The elastic modulus of BFRP rebar at 70 GPa is much lower than that of steel at 200 GPa, which leads to excessive deformation at the service limit compared to steel bars, if the same cross-sectional area is used [201,202]. Therefore, concrete reinforced with BFRP rebar shows more flexural and shear cracking than when steel is used [203]. However, compared to steel, BFRP rebar does not exhibit yielding during tension as the behaviour is purely elastic. The creep of BFRP rebar depends on its own fibre properties, the resin and their bonding with each other.

Elavenil et al. [204] concluded that the creep rupture strength of BFRP rebar is less than their tensile strength, when compared to that of steel. Tomlinson and Fam [205] showed that standard design methods predicted well the failing of beams reinforced with BFRP rebar in flexure, but for failing in shear a modified compression field theory was required. Although some work has been conducted on the use of SCMs in engineered cementitious composites (ECC) in order to reduce CO_2 emissions, the field is underdeveloped [206]. Cai et al. [207] noted that BFRP rebar may be better utilised in ECC than in normal concrete, because ECC has a much better crack controlling ability. Despite the environmental benefit of combining BFRP rebar with AAM, there are limited reports on the structural behaviour of such composites [208].

Despite the lower elastic modulus of BFRP rebar compared to steel, its main advantage is inertness to aggressive chemical conditions. Serbescu et al. [209] showed that BFRP rebar in an aggressive environment is expected to retain 72 to 80% of its strength after 100 years of exposure. BFRP is advantageous when used in structures exposed to saline conditions. While steel rebar will corrode when oxidants and chloride diffuse through the protective concrete cover, or when the pore solution loses its alkalinity owing to carbonation, this becomes irrelevant in the case of BFRP, provided the cementitious phases in the concrete remain stable. Consequently, BFRP rebar requires a thinner concrete cover only for structural reasons rather than to prevent corrosion, which results in a decrease in CO_2 emissions. It is suggested that BFRP rebar should be investigated for application in thin section precast concrete in the first instance.

BFRP rebar does not conduct electricity and is non-magnetic, so airport runways and walkways, communications towers and terminals would not be subject to radio frequency interference as they are now from steel rebar. Moreover, the use of BFRP rebar in marine concrete prevents electrolysis. BFRP is three times lighter than steel rebar, which facilitates easier handling and construction [198].

Inman et al. [198] stated that the energy required for basalt fibre production is around 5 kWh/kg in an electric furnace, while the energy required for steel is around 14 kWh/kg. When Inman et al. [198] accounted for the high CO_2 emission of the epoxy resin, the BFRP and steel rebar had similar emissions, i.e. 2.6 and 2.34 kg CO_2-eq./kg respectively. However, since BFRP is three times lighter than steel, Inman et al. [198] concluded that the overall embodied CO_2 emissions are much lower in concrete reinforced with BFRP rebar than in the case of steel rebar.

As a result of its much lower modulus of elasticity, BFRP rebar is unlikely to replace steel rebar in many structural applications. However, there are numerous applications where BFRP rebar could be a suitable alternative reinforcement, especially under aggressive exposure conditions. The construction industry is conservative, and it takes a very long time to get new methods and materials adopted. It is hoped that the non-corrosive nature of BFRP rebar, its compatibility with cementitious binders with low CO_2 emissions, together with its inherently low CO_2 emissions, will motivate the construction materials industry and research community to give BFRP rebar the attention it deserves.

Roadmap for Low-CO_2 Cement Production

It is evident from a review of the literature that much has already been done on the development of low-CO_2 cement and concrete. However, the implicit assumption in many papers and commercial feasibility studies is that the reaction kinetics of a mix design are dictated by the properties of the source materials, which cannot be changed, unless they are subjected to clinkerisation or calcination type processes. The development of reactor systems like EESS makes it possible to modify source material properties chemically and physically, which creates an opportunity to utilise secondary and virgin materials that currently have limited value. As suggested above, this development demands a

rethinking of the cementitious value chain. Industries like information technology, biotechnology, space, energy generation, transportation, and finance have experienced radical innovation, while the bulk material processing industries, including cement and concrete, have largely experienced incremental innovation. It is recognised that radical innovation in most industries has originated from entrepreneurs outside the incumbent players. Over time, it will be noteworthy to see whether the cement and concrete industry is an exception. A roadmap contemplating radical innovation in the cementitious value chain must contemplate the inevitable obstacles in parallel with the opportunities.

Roadmap for Research

This article has identified numerous gaps in our knowledge and opportunities for research. Most companies conduct research relevant to their immediate production needs, with only a small portion of funding allocated to blue sky research. On the other hand, universities are supposed to conduct more blue sky research, usually funded by competitive grants from government agencies. In an attempt to make research more relevant to industrial practice, governments are increasingly allocating research funding to collaborative projects between multiple universities and companies contributing matching funding. Expectedly, this trend skews research to the needs identified by large industry players, because entrepreneurs usually do not have the means to contribute matching funding. Furthermore, a key objective of university research is to educate students and young researchers, with the success of projects being assessed by the quality of journal papers published. Inevitably, this system rarely focuses on radical innovation in the industrial players that co-fund the research. Therefore, university-based research on cementitious materials faces a substantial risk of not meeting the needs of a roadmap for shifting the cement industry to low-CO_2 production.

Figure 8 gives a conceptual diagram of research subjects in this area that deserve attention. Much research has been focused on binding phase formation and mechanisms, but without contemplating the options for a transformation of material properties. Surface chemistry has been neglected and offers rich opportunity, but it is a challenge how such work will be funded, especially when the synthesis of plasticisers is expensive and tedious work. There is an urgent need for models to predict service life of concrete, and to link such models to microstructural phenomena and exposure conditions. A major area of research that has been largely neglected is the relationship between microstructure and macro-engineering behaviour. Arguably, material scientists interested in microstructure are less interested in structural engineering design, while structural engineers are less familiar with materials science and use largely empirical correlations for design. Confidence in the design equations for concrete incorporating new binders or source materials is essential before structural engineers will be willing to approve designs. In addition, structural engineers need to be confident about the physical and chemical durability of a new concrete. This issue is one of the major obstacles in the commercial adoption of low CO_2 cements and sadly, receives little attention by the research community and industry incumbents.

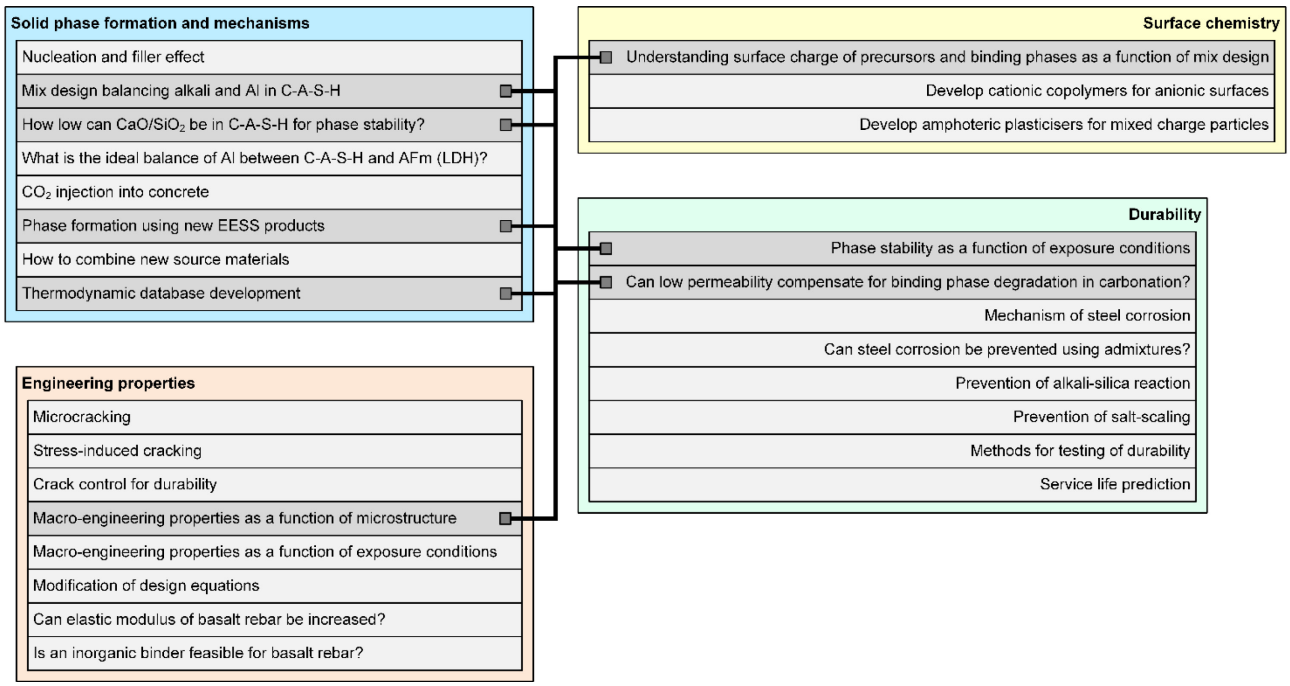

Figure 8. Interrelationship between research subjects requiring attention in the production of low-CO_2 cement and concrete

The case for performance-based standards

In view of the low reactivity of GBS and FA relative to PC, the regulatory framework for cement and concrete in most jurisdictions has remained prescriptive, even when it is claimed superficially that such standards are performance-based. The committees drafting such standards usually have good intentions to ensure quality of concrete, but in the process, may not be aware of the constraints they place on innovation by basing their assumptions on the chemistry of conventional PC blends without taking into account the fundamentals governing the chemistry of AAM and PC blends with high SCM content. In essence, the standards frameworks often restrict the content of GBS, FA, ground limestone, and calcined clay, and hence prescribe concrete compositions. Moreover, the definitions of GBS and FA are often so narrow that it is not possible to utilise source materials that are not already in the cementitious supply chain, which is often controlled by industry incumbents. An example of the reluctance of the construction materials industry to adopt performance-based standards is ASTM C1157 published in 1992, which was subsequently not accepted by ACI 301 and 318 concrete codes, and not accepted by 29 out of 35 departments of transport in the United States [210].

If a reactor (e.g., EESS) is used to transform source material properties into a form that is not PC clinker, but still reactive and effective in forming durable binding phases, the reaction products will likely not meet the standards in most jurisdictions. Structural engineers ask the simple question: "Does the new cement/concrete meet the standard?" A conditional response is unconvincing and then the product does not proceed to large scale commercial adoption, apart from more limited demonstration projects. Zeobond in Australia has had extensive experience with implementation of AAM in demonstration projects and some larger commercial applications, despite a restrictive standards regime; success has been achieved by close collaboration with asset owners, architects, structural engineers, the community, and regulatory authorities [151,211-215]. A similar approach of participation by the various stakeholders will be required to get cementitious products from alternative reactors adopted. Only through such demonstration projects will standards committee members become convinced of the merits of new materials. The risk is that industry incumbents

may object out of self-interest if proposed changes in standards are to the detriment of the existing industry, because standards committees are highly political despite claims to the contrary.

In order to enable the wide adoption of low-CO_2 cement and concrete using alternative reactor technologies like EESS, it is essential that a performance-based standards framework be adopted instead of the current prescriptive system. At the least, such a performance-based framework should apply to concretes containing above the maximum SCM currently specified. There should be no restriction on the type of components used, either as cementitious material, aggregates or admixtures/activators. The amount of cementitious material and the water/cement ratio should also not be restricted. Suppliers should report the content of PC and other SCM, but for commercial reasons the specific nature of the admixtures/activators do not need to be specified. A material safety data sheet (MSDS) should of course be supplied for all admixtures and activators, or combinations thereof. For a dry one-part activated cement mix it may be required to specify only the main components such as an XRF analysis, plus an MSDS.

It is important to ask which performance and durability testing methods should be used in order to specify performance criteria. The discussion above shows the challenge of developing testing methods for durability that are independent of initial binder phase assemblage. In a critical review of performance-based approaches, Alexander and Thomas [216] explained that it is possible to relate service-life prediction models to durability testing, even when it is known that the diffusion parameters in concrete are complicated by several factors, including interaction between the diffusing species and the matrix, and the reduction of diffusion coefficients with age.

It is noteworthy that the Swiss Standard on "Concrete Structures – Complementary Specifications" has adopted the Torrent method based on the coefficient of air-permeability, which has been demonstrated to correlate well with other durability criteria such as water sorptivity and chloride migration for new and aged concrete, as determined on-site [217]. Equally, the South African Durability Index approach involves characterising concrete in-situ and/or on laboratory specimens by using the Oxygen Permeability Index (OPI), water sorptivity, and chloride conductivity, which are then linked to service-life models for the relevant deterioration mechanisms in reinforced concrete structures [19]. Beushausen et al. [217] described how the South African Durability Index has been used in the design of large national infrastructure projects since 2005. They also demonstrated that the Torrent method and the OPI correlate well when applied to the same concrete samples, and both manage to place concrete samples in the same acceptance classes [217]. The above performance criteria may be expanded to include the slump and setting time, and for certain exposure conditions resistance to freeze-thaw, salt scaling, sulphate, acids, and ASR [218]. There is increasing support for a performance-based approach in cement and concrete standards instead of the restrictive prescriptive style in use [19,218,210].

Strategy for commercialisation

Figure 9 outlines a conceptual flow diagram of the various steps and driving forces for the wider commercial adoption of low-CO_2 cement and concrete. As stated above, the commercialisation pathway has many obstacles, including the prescriptive standards regime. Zeobond's experience in Australia has been that changes to the standards regime proceed only when multiple demonstration projects have been completed using special permission to operate outside the standards. This is tedious and expensive work. Even when the standards have been changed to allow for a new cementitious material, structural engineers are reluctant to take risks affecting their professional liability insurance. Equally, the operators of pre-mix and pre-cast concrete plant are reluctant to accept the risk of delivering a new type of cement.

The strategy to overcome this hurdle is to internalise the various steps involving transfer of risk, therefore vertical integration should be advocated. Although the EESS processing may be conducted within an independent entity, it will preferably be conducted within a joint venture between the producer of the residue or other source materials, the cementitious powder producer, the wet concrete manufacturer and a construction company. The final product delivered from this value chain is a concrete structure, not a cement binder or wet concrete. The approach currently followed in the construction materials industry means that risk is outsourced, transferring ultimate responsibility of the respective end use products to other parties. Unfortunately, that approach inhibits innovation and investment into an unproven technology. Instead, the company identifying new source materials should be responsible for their processing and conversion into a cement and/or SCM. By collaborating with independent pre-mix and pre-cast concrete producers, they could be sub-contracted to deliver a new concrete without taking on the liability, which becomes a strong incentive for market expansion. By installing cementitious silos at the sub-contracted concrete producer, the capital risk is also on the material supplier. Likewise, the placement of wet concrete or the building of a concrete structure can be arranged such that the original material supplier retains the risk. It may appear that the internal risk taken on by the material producer is unacceptable; however, each step of risk adoption can accompany an increase in profit margin. The logistics of material transport is a key element protecting industry incumbents from newcomers. It is essential that the company developing new cementitious materials controls its own, independent supply chain and logistical system. By using a distributed processing system, new market opportunities in more remote locations become available.

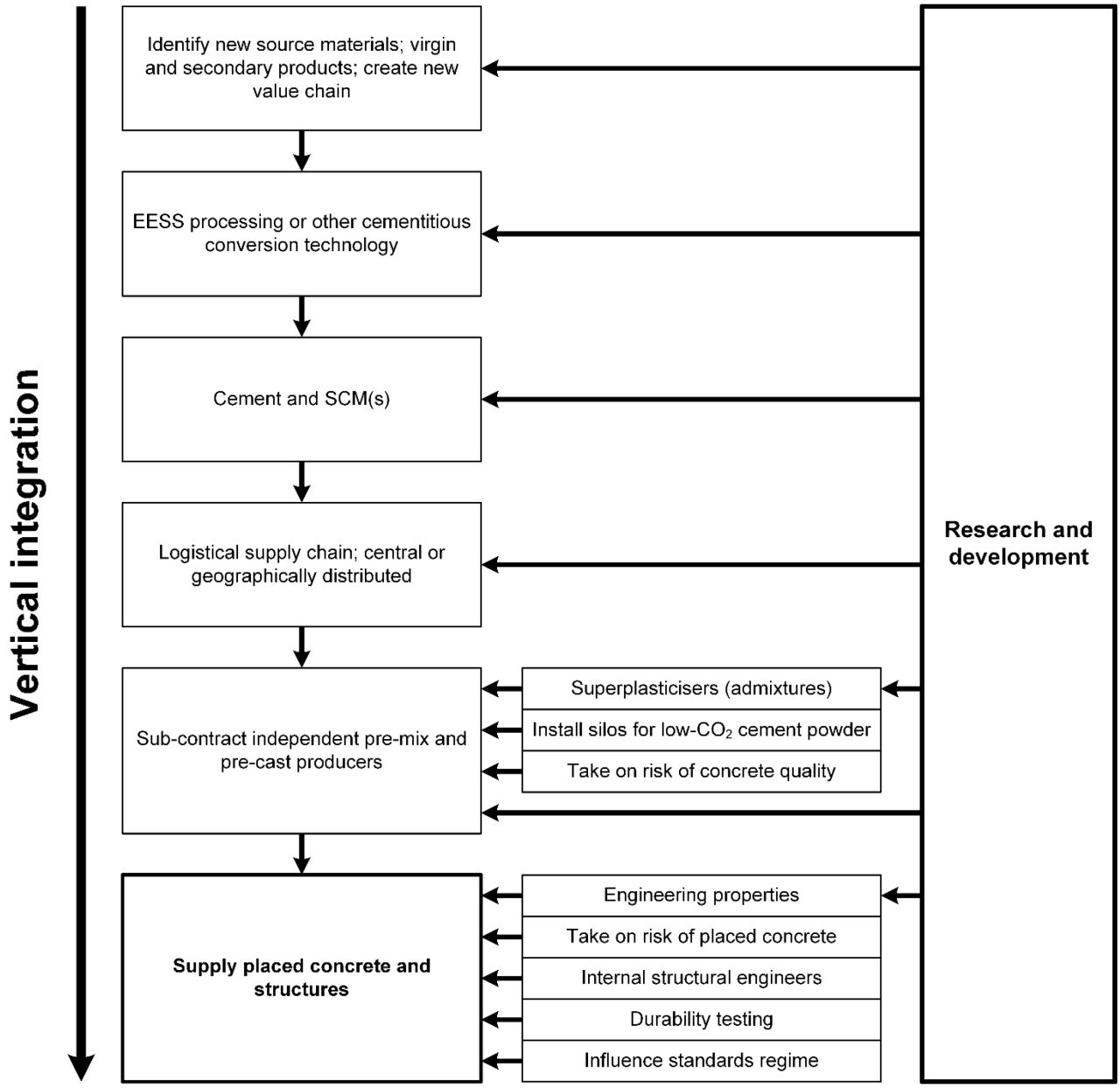

Figure 9. Conceptual diagram for the commercial adoption of low-CO_2 cement and concrete

Besides taking on risk, the main cementitious material supplier should also ensure that structural engineering design is internalised to minimise risk and maintain quality control. The material supplier should also focus on the quantification and modelling of engineering properties as a function of microstructure and thermodynamic phase prediction, in addition to the synthesis of new plasticisers. There should also be an in-depth understanding of factors affecting durability, how durability is tested, and then used to predict service life. This comprehensive approach of vertical integration has been followed rarely, but it will be mandatory if low-CO_2 cements in construction and the built environment are to become mainstream.

Unfortunately, many start-up companies in the field of low-CO_2 cements have not survived. Investors and even successful entrepreneurs in other areas have underestimated the barriers to entry into the cementitious value chain, and the scale of infrastructure that is required to be cost-competitive. The more consolidated the construction materials industry, the more difficult it is for a new entrant to compete. A substantial reduction in CO_2 emissions has not been a sufficient driver for the adoption of new binders or the survival of a new cement business. Moreover, the availability

of an industrial residue for conversion to a cementitious material, in competition with the disposal of such residue, has not been a sufficient driver for its adoption in the cementitious value chain. Some may argue that the business case is simply not there for it to happen, otherwise incumbent cement companies would have shifted to low CO_2 cements and would have utilised more of such residues. New material processing technology as outlined above has the potential to disrupt the existing cementitious value chain, so it can be expected that incumbents would defend the barriers to entry. The business case for the valorisation of industrial residue will become apparent only when entrepreneurs have succeeded in establishing a new value chain for low-CO_2 cements and at the same time have overcome these barriers to entry. *Disruptive innovation* of an industry, as defined by the late Professor Clayton Christensen of the Harvard Business School, is usually driven by new entrants with a different mindset, so it will be unusual for the construction materials industry to follow a different pathway towards a low-CO_2 future.

Acknowledgements

RJM acknowledges funding provided by the Engineering and Physical Sciences Research Council of the U.K. (EP/S006079/1). The research leading to this publication benefitted from EPSRC funding under grant No. EP/R010161/1 and from support from the UKCRIC Coordination Node, EPSRC grant number EP/R017727/1, which funds UKCRIC's ongoing coordination. CEW acknowledges financial support from Grant Nos. 1362039 and 1553607 and the MRSEC Center (Grant No. DMR-1420541) from the National Science Foundation, USA. Access to the Princeton Institute for Computational Science and Engineering (PICSciE) and the Office of Information Technology's High Performance Computing Center and Visualization Laboratory at Princeton University is acknowledged. Unpublished pore structure and permeability data were obtained and analysed by Kengran Yang, Anna Blyth and Bridget Zakrzewski (Princeton University).

Conflict of Interest

Jannie S.J. van Deventer declares a conflict of interest through the commercial application of electrically-enhanced supersonic shockwave reactors for the processing of minerals, secondary sources and cementitious materials. RJM and CEW declare no conflict of interest.

References

1. United Nations Department of Economic and Social Affairs: World population prospects 2019. https://population.un.org/wpp/. Accessed 6 February 2020
2. GCP Global: Global construction 2030: A global forecast for the construction industry to 2030. https://gcp.global/uk/products/global-construction-2030/ (2015).
3. Schneider, M.: The cement industry on the way to a low-carbon future. Cement and Concrete Research **124**, 105792 (2019). doi:https://doi.org/10.1016/j.cemconres.2019.105792
4. IPCC (ed.) Climate change 2014: Synthesis report. IPCC, Geneva (2014)
5. Ellis, L.D., Badel, A.F., Chiang, M.L., Park, R.J.-Y., Chiang, Y.-M.: Toward electrochemical synthesis of cement—an electrolyzer-based process for decarbonating caco₃ while producing useful gas streams. P. Natl. Acad. Sci. USA, 201821673 (2019). doi:10.1073/pnas.1821673116
6. Beyond Zero Emissions: Zero carbon industry plan, rethinking cement. https://bze.org.au/research/manufacturing-industrial-processes/rethinking-cement/ (2017). Accessed 6 February 2020
7. Chatterjee, A., Sui, T.: Alternative fuels – effects on clinker process and properties. Cement and Concrete Research **123**, 105777 (2019). doi:https://doi.org/10.1016/j.cemconres.2019.105777

8. Moranville-Regourd, M., BKamali-Bernard, S.: Cements from blastfurnace slag. In: Hewlett, P.C., Liska, M. (eds.) Lea's chemistry of cement and concrete. (2019)
9. Juenger, M.C.G., Snellings, R., Bernal, S.A.: Supplementary cementitious materials: New sources, characterization, and performance insights. Cement and Concrete Research **122**, 257-273 (2019). doi:https://doi.org/10.1016/j.cemconres.2019.05.008
10. Skibsted, J., Snellings, R.: Reactivity of supplementary cementitious materials (scms) in cement blends. Cement and Concrete Research **124**, 105799 (2019). doi:https://doi.org/10.1016/j.cemconres.2019.105799
11. Giergiczny, Z.: Fly ash and slag. Cement and Concrete Research **124**, 105826 (2019). doi:https://doi.org/10.1016/j.cemconres.2019.105826
12. Provis, J.L., Palomo, A., Shi, C.: Advances in understanding alkali-activated materials. Cement and Concrete Research **78A**, 110-125 (2015). doi:http://dx.doi.org/10.1016/j.cemconres.2015.04.013
13. Provis, J.L.: Alkali-activated materials. Cement and Concrete Research **114**, 40-48 (2018). doi:https://doi.org/10.1016/j.cemconres.2017.02.009
14. Shi, C., Qu, B., Provis, J.L.: Recent progress in low-carbon binders. Cement and Concrete Research **122**, 227-250 (2019). doi:https://doi.org/10.1016/j.cemconres.2019.05.009
15. Palomo, A., Monteiro, P., Martauz, P., Bilek, V., Fernandez-Jimenez, A.: Hybrid binders: A journey from the past to a sustainable future (opus caementicium futurum). Cement and Concrete Research **124**, 105829 (2019). doi:https://doi.org/10.1016/j.cemconres.2019.105829
16. Scrivener, K., Martirena, F., Bishnoi, S., Maity, S.: Calcined clay limestone cements (lc3). Cement and Concrete Research **114**, 49-56 (2018). doi:https://doi.org/10.1016/j.cemconres.2017.08.017
17. Geng, G., Myers, R.J., Qomi, M.J.A., Monteiro, P.J.M.: Densification of the interlayer spacing governs the nanomechanical properties of calcium-silicate-hydrate. Sci. Rep. **7**(1), 10986 (2017). doi:10.1038/s41598-017-11146-8
18. Scrivener, K.L., Juilland, P., Monteiro, P.J.M.: Advances in understanding hydration of portland cement. Cement and Concrete Research **78A**, 38-56 (2015). doi:http://dx.doi.org/10.1016/j.cemconres.2015.05.025
19. Alexander, M., Beushausen, H.: Durability, service life prediction, and modelling for reinforced concrete structures – review and critique. Cement and Concrete Research **122**, 17-29 (2019). doi:https://doi.org/10.1016/j.cemconres.2019.04.018
20. Jennings, H.M., Bullard, J.W.: From electrons to infrastructure: Engineering concrete from the bottom up. Cement and Concrete Research **41**(7), 727-735 (2011). doi:http://dx.doi.org/10.1016/j.cemconres.2011.03.025
21. Bullard, J.W., Lothenbach, B., Stutzman, P.E., Snyder, K.A.: Coupling thermodynamics and digital image models to simulate hydration and microstructure development of portland cement pastes. Journal of Materials Research **26**(4), 609-622 (2011).
22. Damidot, D., Lothenbach, B., Herfort, D., Glasser, F.P.: Thermodynamics and cement science. Cement and Concrete Research **41**(7), 679-695 (2011).
23. Atkins, M., Bennett, D.G., Dawes, A.C., Glasser, F.P., Kindness, A., Read, D.: A thermodynamic model for blended cements. Cement and Concrete Research **22**(2–3), 497-502 (1992). doi:http://dx.doi.org/10.1016/0008-8846(92)90093-B
24. Reardon, E.J.: An ion interaction model for the determination of chemical equilibria in cement/water systems. Cement and Concrete Research **20**(2), 175-192 (1990). doi:http://dx.doi.org/10.1016/0008-8846(90)90070-E
25. Lothenbach, B., Winnefeld, F.: Thermodynamic modelling of the hydration of portland cement. Cement and Concrete Research **36**(2), 209-226 (2006).
26. Berner, U.R.: Evolution of pore water chemistry during degradation of cement in a radioactive waste repository environment. Waste Manage. **12**(2–3), 201-219 (1992). doi:http://dx.doi.org/10.1016/0956-053X(92)90049-O

27. Sui, S., Georget, F., Maraghechi, H., Sun, W., Scrivener, K.: Towards a generic approach to durability: Factors affecting chloride transport in binary and ternary cementitious materials. Cement and Concrete Research **124**, 105783 (2019). doi:https://doi.org/10.1016/j.cemconres.2019.105783
28. Azad, V.J., Li, C., Verba, C., Ideker, J.H., Isgor, O.B.: A comsol–gems interface for modeling coupled reactive-transport geochemical processes. Computers & Geosciences **92**, 79-89 (2016). doi:https://doi.org/10.1016/j.cageo.2016.04.002
29. Helgeson, H.C., Kirkham, D.H., Flowers, G.C.: Theoretical prediction of the thermodynamic behavior of aqueous electrolytes at high pressures and temperatures: Iv. Calculation of activity coefficients, osmotic coefficients, and apparent molal and standard and relative partial molal properties to 600°c and 5 kb. American Journal of Science **281**(10), 1249-1516 (1981).
30. Kulik, D.A., Wagner, T., Dmytrieva, S.V., Kosakowski, G., Hingerl, F.F., Chudnenko, K.V., Berner, U.: Gem-selektor geochemical modeling package: Revised algorithm and gems3k numerical kernel for coupled simulation codes. Comput. Geosci. **17**(1), 1-24 (2013). doi:10.1007/s10596-012-9310-6
31. Anderson, G.M., Crerar, D.A.: Thermodynamics in geochemistry: The equilibrium model. Oxford University Press, Oxford (1993)
32. Myers, R.J., Bernal, S.A., Provis, J.L.: A thermodynamic model for c-(n-)a-s-h gel: Cnash_ss. Derivation and application. Cement and Concrete Research **66**, 27-47 (2014). doi:10.1016/j.cemconres.2014.1007.1005
33. Rothstein, D., Thomas, J.J., Christensen, B.J., Jennings, H.M.: Solubility behavior of ca-, s-, al-, and si-bearing solid phases in portland cement pore solutions as a function of hydration time. Cement and Concrete Research **32**(10), 1663-1671 (2002). doi:http://dx.doi.org/10.1016/S0008-8846(02)00855-4
34. Pitzer, K.S.: Thermodynamics of electrolytes. I. Theoretical basis and general equations. The Journal of Physical Chemistry **77**(2), 268-277 (1973). doi:10.1021/j100621a026
35. Lothenbach, B., Kulik, D.A., Matschei, T., Balonis, M., Baquerizo, L., Dilnesa, B., Miron, G.D., Myers, R.J.: Cemdata18: A chemical thermodynamic database for hydrated portland cements and alkali-activated materials. Cement and Concrete Research **115**, 472-506 (2019). doi:https://doi.org/10.1016/j.cemconres.2018.04.018
36. Kulik, D.A.: Improving the structural consistency of c-s-h solid solution thermodynamic models. Cement and Concrete Research **41**(5), 477-495 (2011).
37. Myers, R.J., Bernal, S.A., Provis, J.L.: A thermodynamic model for c-(n-)a-s-h gel: Cnash_ss. Derivation and validation. Cement and Concrete Research **66**, 27-47 (2014). doi:https://doi.org/10.1016/j.cemconres.2014.07.005
38. Matschei, T., Lothenbach, B., Glasser, F.P.: Thermodynamic properties of portland cement hydrates in the system cao-al_2o_3-sio_2-$caso_4$-$caco_3$-h_2o. Cement and Concrete Research **37**(10), 1379-1410 (2007).
39. Blanc, P., Bourbon, X., Lassin, A., Gaucher, E.C.: Chemical model for cement-based materials: Temperature dependence of thermodynamic functions for nanocrystalline and crystalline c-s-h phases. Cement and Concrete Research **40**(6), 851-866 (2010).
40. Arthur, R., Sasamoto, H., Walker, C., Yui, M.: Polymer model of zeolite thermochemical stability. Clay Clay Miner. **59**(6), 626-639 (2011). doi:10.1346/ccmn.2011.0590608
41. Durdziński, P.T., Ben Haha, M., Bernal, S.A., De Belie, N., Gruyaert, E., Lothenbach, B., Menéndez Méndez, E., Provis, J.L., Schöler, A., Stabler, C., Tan, Z., Villagrán Zaccardi, Y., Vollpracht, A., Winnefeld, F., Zając, M., Scrivener, K.L.: Outcomes of the rilem round robin on degree of reaction of slag and fly ash in blended cements. Materials and Structures **50**(2), 135 (2017). doi:10.1617/s11527-017-1002-1
42. Kocaba, V., Gallucci, E., Scrivener, K.L.: Methods for determination of degree of reaction of slag in blended cement pastes. Cement and Concrete Research **42**(3), 511-525 (2012).

43. Lothenbach, B., Xu, B., Winnefeld, F.: Thermodynamic data for magnesium (potassium) phosphates. Appl. Geochem. **111**, 104450 (2019). doi:https://doi.org/10.1016/j.apgeochem.2019.104450
44. Bernard, E., Lothenbach, B., Cau-Dit-Coumes, C., Pochard, I., Rentsch, D.: Aluminum incorporation into magnesium silicate hydrate (m-s-h). Cement and Concrete Research **128**, 105931 (2020). doi:https://doi.org/10.1016/j.cemconres.2019.105931
45. Gomez-Zamorano, L., Balonis, M., Erdemli, B., Neithalath, N., Sant, G.: C–(n)–s–h and n–a–s–h gels: Compositions and solubility data at 25°c and 50°c. Journal of the American Ceramic Society **100**(6), 2700-2711 (2017). doi:10.1111/jace.14715
46. Environment, U., Scrivener, K.L., John, V.M., Gartner, E.M.: Eco-efficient cements: Potential economically viable solutions for a low-co_2 cement-based materials industry. Cement and Concrete Research **114**, 2-26 (2018). doi:https://doi.org/10.1016/j.cemconres.2018.03.015
47. Duchesne, J., Bérubé, M.A.: Effect of supplementary cementing materials on the composition of cement hydration products. Advanced Cement Based Materials **2**(2), 43-52 (1995). doi:https://doi.org/10.1016/1065-7355(95)90024-1
48. Taylor, H.F.W.: Nanostructure of c-s-h: Current status. Advanced Cement Based Materials **1**(1), 38-46 (1993). doi:https://doi.org/10.1016/1065-7355(93)90006-A
49. Durdziński, P.T., Ben Haha, M., Zajac, M., Scrivener, K.L.: Phase assemblage of composite cements. Cement and Concrete Research **99**, 172-182 (2017). doi:https://doi.org/10.1016/j.cemconres.2017.05.009
50. Andersen, M.D., Jakobsen, H.J., Skibsted, J.: Incorporation of aluminum in the calcium silicate hydrate (c−s−h) of hydrated portland cements: A high-field ^{27}al and ^{29}si mas nmr investigation. Inorganic Chemistry **42**(7), 2280-2287 (2003). doi:10.1021/ic020607b
51. He, Z., Qian, C., Zhang, Y., Zhao, F., Hu, Y.: Nanoindentation characteristics of cement with different mineral admixtures. Science China Technological Sciences **56**(5), 1119-1123 (2013). doi:10.1007/s11431-013-5186-5
52. Hu, C., Li, Z.: Property investigation of individual phases in cementitious composites containing silica fume and fly ash. Cement and Concrete Composites **57**, 17-26 (2015). doi:https://doi.org/10.1016/j.cemconcomp.2014.11.011
53. Myers, R.J., Bernal, S.A., Gehman, J.D., van Deventer, J.S.J., Provis, J.L.: The role of al in cross-linking of alkali-activated slag cements. Journal of the American Ceramic Society **98**(3), 996-1004 (2015). doi:10.1111/jace.13360
54. Richardson, I.G., Brough, A.R., Groves, G.W., Dobson, C.M.: The characterization of hardened alkali-activated blast-furnace slag pastes and the nature of the calcium silicate hydrate (c-s-h) phase. Cement and Concrete Research **24**(5), 813-829 (1994).
55. Brough, A.R., Atkinson, A.: Sodium silicate-based, alkali-activated slag mortars: Part i. Strength, hydration and microstructure. Cement and Concrete Research **32**(6), 865-879 (2002). doi:http://dx.doi.org/10.1016/S0008-8846(02)00717-2
56. Fernández-Jiménez, A., Puertas, F., Sobrados, I., Sanz, J.: Structure of calcium silicate hydrates formed in alkaline-activated slag: Influence of the type of alkaline activator. Journal of the American Ceramic Society **86**(8), 1389-1394 (2003). doi:10.1111/j.1151-2916.2003.tb03481.x
57. White, C.E., Daemen, L.L., Hartl, M., Page, K.: Intrinsic differences in atomic ordering of calcium (alumino)silicate hydrates in conventional and alkali-activated cements. Cement and Concrete Research **67**, 66-73 (2015). doi:http://dx.doi.org/10.1016/j.cemconres.2014.08.006
58. Gong, K., White, C.E.: Impact of chemical variability of ground granulated blast-furnace slag on the phase formation in alkali-activated slag pastes. Cement and Concrete Research **89**, 310-319 (2016). doi:http://dx.doi.org/10.1016/j.cemconres.2016.09.003
59. Garg, N., White, C.E.: Mechanism of zinc oxide retardation in alkali-activated materials: An in situ x-ray pair distribution function investigation. J. Mater. Chem. A **5**, 11794-11804 (2017). doi:10.1039/C7TA00412E

60. Kurtis, K.E., Monteiro, P.J.M.: Chemical additives to control expansion of alkali-silica reaction gel: Proposed mechanisms of control. Journal of Materials Science **38**(9), 2027-2036 (2003). doi:10.1023/a:1023549824201
61. Rajabipour, F., Giannini, E., Dunant, C., Ideker, J.H., Thomas, M.D.A.: Alkali–silica reaction: Current understanding of the reaction mechanisms and the knowledge gaps. Cement and Concrete Research **76**, 130-146 (2015). doi:https://doi.org/10.1016/j.cemconres.2015.05.024
62. Shi, Z., Geng, G., Leemann, A., Lothenbach, B.: Synthesis, characterization, and water uptake property of alkali-silica reaction products. Cement and Concrete Research **121**, 58-71 (2019). doi:https://doi.org/10.1016/j.cemconres.2019.04.009
63. Shi, Z., Lothenbach, B.: The combined effect of potassium, sodium and calcium on the formation of alkali-silica reaction products. Cement and Concrete Research **127**, 105914 (2020). doi:https://doi.org/10.1016/j.cemconres.2019.105914
64. Fernández-Jiménez, A., Puertas, F.: The alkali–silica reaction in alkali-activated granulated slag mortars with reactive aggregate. Cement and Concrete Research **32**(7), 1019-1024 (2002). doi:https://doi.org/10.1016/S0008-8846(01)00745-1
65. Shi, C., Shi, Z., Hu, X., Zhao, R., Chong, L.: A review on alkali-aggregate reactions in alkali-activated mortars/concretes made with alkali-reactive aggregates. Materials and Structures **48**(3), 621-628 (2015). doi:10.1617/s11527-014-0505-2
66. Shi, Z., Shi, C., Wan, S., Zhang, Z.: Effects of alkali dosage and silicate modulus on alkali-silica reaction in alkali-activated slag mortars. Cement and Concrete Research **111**, 104-115 (2018). doi:https://doi.org/10.1016/j.cemconres.2018.06.005
67. Shi, Z., Lothenbach, B.: The role of calcium on the formation of alkali-silica reaction products. Cement and Concrete Research **126**, 105898 (2019). doi:https://doi.org/10.1016/j.cemconres.2019.105898
68. Federico, L.M., Chidiac, S.E.: Waste glass as a supplementary cementitious material in concrete – critical review of treatment methods. Cement and Concrete Composites **31**(8), 606-610 (2009). doi:https://doi.org/10.1016/j.cemconcomp.2009.02.001
69. Marija, K., Julio, F.D.: Field application of recycled glass pozzolan for concrete. ACI Materials Journal **116**(4), 123-131 (2019). doi:10.14359/51716716
70. Saccani, A., Bignozzi, M.C.: Asr expansion behavior of recycled glass fine aggregates in concrete. Cement and Concrete Research **40**(4), 531-536 (2010). doi:https://doi.org/10.1016/j.cemconres.2009.09.003
71. Sánchez-Herrero, M.J., Fernández-Jiménez, A., Palomo, Á.: Alkaline hydration of c_2s and c_3s. Journal of the American Ceramic Society **99**(2), 604-611 (2016). doi:10.1111/jace.13985
72. L'Hôpital, E., Lothenbach, B., Scrivener, K., Kulik, D.A.: Alkali uptake in calcium alumina silicate hydrate (c-a-s-h). Cement and Concrete Research **85**, 122-136 (2016). doi:http://dx.doi.org/10.1016/j.cemconres.2016.03.009
73. Myers, R.J., L'Hôpital, E., Provis, J.L., Lothenbach, B.: Composition–solubility–structure relationships in calcium (alkali) aluminosilicate hydrate (c-(n,k-)a-s-h). Dalton Trans. **44**(30), 13530-13544 (2015). doi:10.1039/C5DT01124H
74. Walkley, B., San Nicolas, R., Sani, M.-A., Rees, G.J., Hanna, J.V., van Deventer, J.S.J., Provis, J.L.: Phase evolution of c-(n)-a-s-h/n-a-s-h gel blends investigated via alkali-activation of synthetic calcium aluminosilicate precursors. Cement and Concrete Research **89**, 120-135 (2016). doi:http://dx.doi.org/10.1016/j.cemconres.2016.08.010
75. Vigna, E., Skibsted, J.: Optimization of alkali activated portland cement—calcined clay blends based on phase assemblage in the na_2o–cao–al_2o_3–sio_2–h_2o system. In: Scrivener, K., Favier, A. (eds.) Calcined clays for sustainable concrete Calcined clays for sustainable concrete, pp. 101-107. Springer Netherlands, Dordrecht (2015)
76. García Lodeiro, I., Fernández-Jimenez, A., Palomo, A., Macphee, D.E.: Effect on fresh c-s-h gels of the simultaneous addition of alkali and aluminium. Cement and Concrete Research **40**(1), 27-32 (2010). doi:10.1016/j.cemconres.2009.08.004

77. Bernal, S.A., Mejía de Gutiérrez, R., Pedraza, A.L., Provis, J.L., Rodriguez, E.D., Delvasto, S.: Effect of binder content on the performance of alkali-activated slag concretes. Cement and Concrete Research **41**(1), 1-8 (2011). doi:http://dx.doi.org/10.1016/j.cemconres.2010.08.017
78. Bernal, S.A., Rodríguez, E.D., Mejía de Gutiérrez, R., Gordillo, M., Provis, J.L.: Mechanical and thermal characterisation of geopolymers based on silicate-activated metakaolin/slag blends. Journal of Materials Science **46**(16), 5477-5486 (2011).
79. Collins, F.G., Sanjayan, J.G.: Workability and mechanical properties of alkali activated slag concrete. Cement and Concrete Research **29**(3), 455-458 (1999). doi:https://doi.org/10.1016/S0008-8846(98)00236-1
80. Shi, C.J.: Strength, pore structure and permeability of alkali-activated slag mortars. Cement and Concrete Research **26**(12), 1789-1799 (1996). doi:10.1016/s0008-8846(96)00174-3
81. Puertas, F., Palacios, M., Manzano, H., Dolado, J.S., Rico, A., Rodríguez, J.: A model for the c-a-s-h gel formed in alkali-activated slag cements. Journal of the European Ceramic Society **31**(12), 2043-2056 (2011).
82. Hafner, J.: Ab-initio simulations of materials using vasp: Density-functional theory and beyond. Journal of Computational Chemistry **29**(13), 2044-2078 (2008). doi:10.1002/jcc.21057
83. Jones, R.O.: Density functional theory: Its origins, rise to prominence, and future. Reviews of Modern Physics **87**(3), 897-923 (2015). doi:10.1103/RevModPhys.87.897
84. Skylaris, C.-K.: A benchmark for materials simulation. Science **351**(6280), 1394-1395 (2016). doi:10.1126/science.aaf3412
85. Kumar, A., Walder, B.J., Kunhi Mohamed, A., Hofstetter, A., Srinivasan, B., Rossini, A.J., Scrivener, K., Emsley, L., Bowen, P.: The atomic-level structure of cementitious calcium silicate hydrate. Journal of Physical Chemistry C **121**(32), 17188-17196 (2017). doi:10.1021/acs.jpcc.7b02439
86. Churakov, S.V., Labbez, C.: Thermodynamics and molecular mechanism of al incorporation in calcium silicate hydrates. Journal of Physical Chemistry C **121**(8), 4412-4419 (2017). doi:10.1021/acs.jpcc.6b12850
87. Kunhi Mohamed, A., Parker, S.C., Bowen, P., Galmarini, S.: An atomistic building block description of c-s-h - towards a realistic c-s-h model. Cement and Concrete Research **107**, 221-235 (2018). doi:https://doi.org/10.1016/j.cemconres.2018.01.007
88. Özçelik, V.O., Garg, N., White, C.E.: Symmetry-induced stability in alkali-doped calcium silicate hydrate. Journal of Physical Chemistry C **123**(22), 14081-14088 (2019). doi:10.1021/acs.jpcc.9b04031
89. Özçelik, V.O., White, C.E.: Nanoscale charge-balancing mechanism in alkali-substituted calcium–silicate–hydrate gels. Journal of Physical Chemistry Letters **7**(24), 5266-5272 (2016). doi:10.1021/acs.jpclett.6b02233
90. Hajimohammadi, A., Provis, J.L., van Deventer, J.S.J.: Effect of alumina release rate on the mechanism of geopolymer gel formation. Chemistry of Materials **22**(18), 5199-5208 (2010). doi:10.1021/cm101151n
91. Ben Haha, M., Le Saout, G., Winnefeld, F., Lothenbach, B.: Influence of activator type on hydration kinetics, hydrate assemblage and microstructural development of alkali activated blast-furnace slags. Cem. Concr. Res. **41**(3), 301-310 (2011). doi:http://dx.doi.org/10.1016/j.cemconres.2010.11.016
92. Garg, N., Özçelik, V.O., Skibsted, J., White, C.E.: Nanoscale ordering and depolymerization of calcium silicate hydrates in presence of alkalis. Journal of Physical Chemistry C **in press** (2019).
93. L'Hôpital, E., Lothenbach, B., Le Saout, G., Kulik, D., Scrivener, K.: Incorporation of aluminium in calcium-silicate-hydrates. Cement and Concrete Research **75**, 91-103 (2015). doi:http://dx.doi.org/10.1016/j.cemconres.2015.04.007
94. Davidovits, J.: Geopolymers - inorganic polymeric new materials. J. Therm. Anal. **37**(8), 1633-1656 (1991). doi:10.1007/bf01912193

95. Barbosa, V.F.F., MacKenzie, K.J.D., Thaumaturgo, C.: Synthesis and characterisation of materials based on inorganic polymers of alumina and silica: Sodium polysialate polymers. International Journal of Inorganic Materials **2**(4), 309-317 (2000).
96. White, C.E., Page, K., Henson, N.J., Provis, J.L.: In situ synchrotron x-ray pair distribution function analysis of the early stages of gel formation in metakaolin-based geopolymers. Applied Clay Science **73**, 17-25 (2013).
97. Provis, J.L., Bernal, S.A.: Geopolymers and related alkali-activated materials. Annu. Rev. Mater. Res. **44**(1), 299-327 (2014). doi:doi:10.1146/annurev-matsci-070813-113515
98. Walkley, B., Rees, G.J., San Nicolas, R., van Deventer, J.S.J., Hanna, J.V., Provis, J.L.: New structural model of hydrous sodium aluminosilicate gels and the role of charge-balancing extra-framework al. Journal of Physical Chemistry C **122**(10), 5673-5685 (2018). doi:10.1021/acs.jpcc.8b00259
99. Thomas, J.J., FitzGerald, S.A., Neumann, D.A., Livingston, R.A.: State of water in hydrating tricalcium silicate and portland cement pastes as measured by quasi-elastic neutron scattering. Journal of the American Ceramic Society **84**(8), 1811-1816 (2001). doi:10.1111/j.1151-2916.2001.tb00919.x
100. Duxson, P., Lukey, G.C., van Deventer, J.S.J.: Physical evolution of na-geopolymer derived from metakaolin up to 1000 °c. Journal of Materials Science **42**(9), 3044-3054 (2007).
101. Jiao, D., King, C., Grossfield, A., Darden, T.A., Ren, P.: Simulation of ca^{2+} and mg^{2+} solvation using polarizable atomic multipole potential. Journal of Physical Chemistry B **110**(37), 18553-18559 (2006). doi:10.1021/jp062230r
102. Kutus, B., Gácsi, A., Pallagi, A., Pálinkó, I., Peintler, G., Sipos, P.: A comprehensive study on the dominant formation of the dissolved $ca(oh)_2(aq)$ in strongly alkaline solutions saturated by ca(ii). RSC Advances **6**(51), 45231-45240 (2016). doi:10.1039/C6RA05337H
103. Properties of the elements & inorganics. In: Rumble, J.R. (ed.) Crc handbook of chemistry and physics, 100th edition (internet version 2019). CRC Press/Taylor & Francis, Boca Raton, FL
104. Scherer, G.W., Valenza II, J.J., Simmons, G.: New methods to measure liquid permeability in porous materials. Cement and Concrete Research **37**(3), 386-397 (2007). doi:http://dx.doi.org/10.1016/j.cemconres.2006.09.020
105. Blyth, A., Eiben, C.A., Scherer, G.W., White, C.E.: Impact of activator chemistry on permeability of alkali-activated slags. Journal of the American Ceramic Society **100**(10), 4848-4859 (2017). doi:10.1111/jace.14996
106. Ma, Y., Wang, G., Ye, G., Hu, J.: A comparative study on the pore structure of alkali-activated fly ash evaluated by mercury intrusion porosimetry, n_2 adsorption and image analysis. Journal of Materials Science **53**(8), 5958-5972 (2018). doi:10.1007/s10853-017-1965-x
107. White, C.E.: Alkali-activated materials: The role of molecular-scale research and lessons from the energy transition to combat climate change RILEM Technical Letters (submitted).
108. Provis, J.L., Myers, R.J., White, C.E., Rose, V., van Deventer, J.S.J.: X-ray microtomography shows pore structure and tortuosity in alkali-activated binders. Cement and Concrete Research **42**(6), 855-864 (2012).
109. Ma, Y., Hu, J., Ye, G.: The pore structure and permeability of alkali activated fly ash. Fuel **104**, 771-780 (2013). doi:https://doi.org/10.1016/j.fuel.2012.05.034
110. Sun, Z., Scherer, G.W.: Pore size and shape in mortar by thermoporometry. Cement and Concrete Research **40**(5), 740-751 (2010). doi:https://doi.org/10.1016/j.cemconres.2009.11.011
111. Abell, A.B., Willis, K.L., Lange, D.A.: Mercury intrusion porosimetry and image analysis of cement-based materials. Journal of Colloid and Interface Science **211**(1), 39-44 (1999). doi:https://doi.org/10.1006/jcis.1998.5986
112. Shi, C.: Strength, pore structure and permeability of alkali-activated slag mortars. Cement and Concrete Research **26**(12), 1789-1799 (1996).
113. Xu, H., Provis, J.L., van Deventer, J.S.J., Krivenko, P.V.: Characterization of aged slag concretes. ACI Materials Journal **105**(2), 131-139 (2008).

114. Buchwald, A., Vanooteghem, M., Gruyaert, E., Hilbig, H., De Belie, N.: Purdocement: Application of alkali-activated slag cement in belgium in the 1950s. Materials and Structures **48**(1), 501-511 (2015). doi:10.1617/s11527-013-0200-8
115. Dufresne, A., Arayro, J., Zhou, T., Ioannidou, K., Ulm, F.-J., Pellenq, R., Béland, L.K.: Atomistic and mesoscale simulation of sodium and potassium adsorption in cement paste. The Journal of Chemical Physics **149**(7), 074705 (2018). doi:10.1063/1.5042755
116. Garg, N., Özçelik, V.O., Skibsted, J., White, C.E.: Nanoscale ordering and depolymerization of calcium silicate hydrates in presence of alkalis. Journal of Physical Chemistry C **123**(40), 24873-24883 (2019).
117. Lothenbach, B., Zajac, M.: Application of thermodynamic modelling to hydrated cements. Cement and Concrete Research **123**, 105779 (2019). doi:https://doi.org/10.1016/j.cemconres.2019.105779
118. Keyte, L.: What's wrong with tarong? The importance of coal fly ash glass chemistry in inorganic polymer synthesis. The University of Melbourne (2008)
119. Kinnunen, P., Sreenivasan, H., Cheeseman, C.R., Illikainen, M.: Phase separation in alumina-rich glasses to increase glass reactivity for low-co2 alkali-activated cements. Journal of Cleaner Production **213**, 126-133 (2019). doi:https://doi.org/10.1016/j.jclepro.2018.12.123
120. Suraneni, P., Palacios, M., Flatt, R.J.: New insights into the hydration of slag in alkaline media using a micro-reactor approach. Cement and Concrete Research **79**, 209-216 (2016). doi:http://dx.doi.org/10.1016/j.cemconres.2015.09.015
121. Scrivener, K., Ouzia, A., Juilland, P., Kunhi Mohamed, A.: Advances in understanding cement hydration mechanisms. Cement and Concrete Research **124**, 105823 (2019). doi:https://doi.org/10.1016/j.cemconres.2019.105823
122. Rees, C.A., Provis, J.L., Lukey, G.C., van Deventer, J.S.J.: The mechanism of geopolymer gel formation investigated through seeded nucleation. Colloid. Surface. A **318**(1), 97-105 (2008). doi:https://doi.org/10.1016/j.colsurfa.2007.12.019
123. Hajimohammadi, A., Provis, J.L., van Deventer, J.S.J.: Time-resolved and spatially-resolved infrared spectroscopic observation of seeded nucleation controlling geopolymer gel formation. Journal of Colloid and Interface Science **357**(2), 384-392 (2011).
124. Berodier, E., Scrivener, K.: Understanding the filler effect on the nucleation and growth of c-s-h. Journal of the American Ceramic Society **97**(12), 3764-3773 (2014). doi:10.1111/jace.13177
125. Ouyang, X., Koleva, D.A., Ye, G., van Breugel, K.: Insights into the mechanisms of nucleation and growth of c–s–h on fillers. Materials and Structures **50**(5), 213 (2017). doi:10.1617/s11527-017-1082-y
126. Bellmann, F., Stark, J.: Activation of blast furnace slag by a new method. Cement and Concrete Research **39**(8), 644-650 (2009). doi:https://doi.org/10.1016/j.cemconres.2009.05.012
127. Monkman, S., MacDonald, M., Hooton, R.D., Sandberg, P.: Properties and durability of concrete produced using co2 as an accelerating admixture. Cement and Concrete Composites **74**, 218-224 (2016). doi:https://doi.org/10.1016/j.cemconcomp.2016.10.007
128. Plank, J., Sakai, E., Miao, C.W., Yu, C., Hong, J.X.: Chemical admixtures — chemistry, applications and their impact on concrete microstructure and durability. Cement and Concrete Research **78**, 81-99 (2015). doi:https://doi.org/10.1016/j.cemconres.2015.05.016
129. Cheung, J., Roberts, L., Liu, J.: Admixtures and sustainability. Cement and Concrete Research **114**, 79-89 (2018). doi:https://doi.org/10.1016/j.cemconres.2017.04.011
130. Liu, J., Yu, C., Shu, X., Ran, Q., Yang, Y.: Recent advance of chemical admixtures in concrete. Cement and Concrete Research **124**, 105834 (2019). doi:https://doi.org/10.1016/j.cemconres.2019.105834
131. Lowke, D., Gehlen, C.: Effect of pore solution composition on zeta potential and superplasticizer adsorption. ACI Symposium Publication **302**.

132. Ersoy, B., Dikmen, S., Uygunoğlu, T., İçduygu Mehmet, G., Kavas, T., Olgun, A.: Effect of mixing water types on the time-dependent zeta potential of portland cement paste. In: Science and Engineering of Composite Materials, vol. 20. vol. 3, p. 285. (2013)
133. Elakneswaran, Y., Nawa, T., Kurumisawa, K.: Zeta potential study of paste blends with slag. Cement and Concrete Composites **31**(1), 72-76 (2009). doi:https://doi.org/10.1016/j.cemconcomp.2008.09.007
134. Kraus, A., Mitkina, T., Dierschke, F., Pulkin, M., Nicoleau, L.: Cationic polymers. US Patent No. 2016/03699024A1,
135. Kashani, A., Provis, J.L., Qiao, G.G., van Deventer, J.S.J.: The interrelationship between surface chemistry and rheology in alkali activated slag paste. Construction and Building Materials **65**, 583-591 (2014). doi:https://doi.org/10.1016/j.conbuildmat.2014.04.127
136. Khayat, K.H., Meng, W., Vallurupalli, K., Teng, L.: Rheological properties of ultra-high-performance concrete — an overview. Cement and Concrete Research **124**, 105828 (2019). doi:https://doi.org/10.1016/j.cemconres.2019.105828
137. Ng, S., Justness, H.: Influence of plasticizers on the rheology and early heat of hydration of blended cements with high content of fly ash. Cement and Concrete Composites **65**, 41-54 (2016).
138. Kashani, A., San Nicolas, R., Qiao, G.G., van Deventer, J.S.J., Provis, J.L.: Modelling the yield stress of ternary cement–slag–fly ash pastes based on particle size distribution. Powder Technology **266**, 203-209 (2014). doi:https://doi.org/10.1016/j.powtec.2014.06.041
139. Stecher, J., Plank, J.: Novel concrete superplasticizers based on phosphate esters. Cement and Concrete Research **119**, 36-43 (2019). doi:https://doi.org/10.1016/j.cemconres.2019.01.006
140. Akhlaghi, O., Menceloglu, Y.Z., Akbulut, O.: Poly(carboxylate ether)-based superplasticizer achieves workability retention in calcium aluminate cement. Sci. Rep. **7**(1), 41743 (2017). doi:10.1038/srep41743
141. Keulen, A., Yu, Q.L., Zhang, S., Grünewald, S.: Effect of admixture on the pore structure refinement and enhanced performance of alkali-activated fly ash-slag concrete. Construction and Building Materials **162**, 27-36 (2018). doi:https://doi.org/10.1016/j.conbuildmat.2017.11.136
142. Marchon, D., Sulser, U., Eberhardt, A., Flatt, R.J.: Molecular design of comb-shaped polycarboxylate dispersants for environmentally friendly concrete. Soft Matter **9**(45), 10719-10728 (2013). doi:10.1039/C3SM51030A
143. Conte, T., Plank, J.: Impact of molecular structure and composition of polycarboxylate comb polymers on the flow properties of alkali-activated slag. Cement and Concrete Research **116**, 95-101 (2019). doi:https://doi.org/10.1016/j.cemconres.2018.11.014
144. Jang, J.G., Lee, N.K., Lee, H.K.: Fresh and hardened properties of alkali-activated fly ash/slag pastes with superplasticizers. Construction and Building Materials **50**, 169-176 (2014). doi:https://doi.org/10.1016/j.conbuildmat.2013.09.048
145. Liu, X.F., Peng, J.H., Wei, G.F., Yang, C.H., Huang, L.Q.: Adsorption characteristics of surfactant on slag in alkali activated slag cement system. Applied Mechanics and Materials **174-177**, 1072-1078 (2012). doi:10.4028/www.scientific.net/AMM.174-177.1072
146. Jacquet, A., Geatches, D.L., Clark, S.J., Greenwell, H.C.: Understanding cationic polymer adsorption on mineral surfaces: Kaolinite in cement aggregates. Minerals **8**(4), 130 (2018).
147. Hampel, C., Zimmermann, J., Alshemari, J., Friederich, M.: Plasticizer having cationic side chains without polyether side chains. US Patent No. 9758608B2
148. Jiang, L., Kong, X., Lu, Z., Hou, S.: Preparation of amphoteric polycarboxylate superplasticizers and their performances in cementitious system. Journal of Applied Polymer Science **132**(4) (2015). doi:10.1002/app.41348
149. Loesche: Compact cement grinding plant (ccg plant). https://www.youtube.com/watch?v=U5n3UnK3oHY (2019). Accessed 6 February 2020
150. Kelsey, C.G., Kelly, J.R.: Super fine crushing - pivotal comminution technology from imp technologies pty. Ltd. In: Impc 2016: Xxviii international mineral processing congress

proceedings. Canadian Institute of Mining, Metallurgy and Petroleum (CIM), Quebec City, Canada (2016)
151. Van Deventer, J.S.J.: Valorisation of slag in construction: So much more than just technology. In: Proceedings of the 5th slag valorisation symposium. Leuven, Belgium (2017)
152. Lansell, P., Keating, W., Lowe, D.: Systems and methods for processing solid materials using shockwaves produced in a supersonic gaseous vortex. US Patent No. 9724703B2,
153. Andres, U.: Electrical disintegration of rock. Mineral Processing and Extractive Metallurgy Review **14**(2), 87-110 (1995). doi:10.1080/08827509508914118
154. de Knoop, L., Juhani Kuisma, M., Löfgren, J., Lodewijks, K., Thuvander, M., Erhart, P., Dmitriev, A., Olsson, E.: Electric-field-controlled reversible order-disorder switching of a metal tip surface. Physical Review Materials **2**(8), 085006 (2018). doi:10.1103/PhysRevMaterials.2.085006
155. San Nicolas, R., Cyr, M., Escadeillas, G.: Characteristics and applications of flash metakaolins. Applied Clay Science **83-84**, 253-262 (2013). doi:https://doi.org/10.1016/j.clay.2013.08.036
156. Long, S., Yan, C., Dong, J.: Microwave-promoted burning of portland cement clinker. Cement and Concrete Research **32**(1), 17-21 (2002). doi:https://doi.org/10.1016/S0008-8846(01)00622-6
157. Snellings, R., Mertens, G., Elsen, J.: Supplementary cementitious materials. Rev. Mineral Geochem. **74**(1), 211-278 (2012). doi:10.2138/rmg.2012.74.6
158. Salman, M., Dubois, M., Maria, A.D., Van Acker, K., Van Balen, K.: Construction materials from stainless steel slags: Technical aspects, environmental benefits, and economic opportunities. J. Ind. Ecol. **20**(4), 854-866 (2016). doi:10.1111/jiec.12314
159. Onisei, S., Pontikes, Y., Van Gerven, T., Angelopoulos, G.N., Velea, T., Predica, V., Moldovan, P.: Synthesis of inorganic polymers using fly ash and primary lead slag. Journal of Hazardous Materials **205-206**, 101-110 (2012). doi:https://doi.org/10.1016/j.jhazmat.2011.12.039
160. Donatello, S., Cheeseman, C.R.: Recycling and recovery routes for incinerated sewage sludge ash (issa): A review. Waste Manage. **33**(11), 2328-2340 (2013). doi:https://doi.org/10.1016/j.wasman.2013.05.024
161. Joseph, A.M., Snellings, R., Van den Heede, P., Matthys, S., De Belie, N.: The use of municipal solid waste incineration ash in various building materials: A belgian point of view. Materials **11**(1), 141 (2018).
162. Scrivener, K., John, V.M., Gartner, E.M.: Eco-efficient cements. Eco-efficient cements: Potential, economically viable solutions for a low-co_2, cement-based materials industry. UNEP, (2016)
163. Snellings, R.: Solution-controlled dissolution of supplementary cementitious material glasses at ph 13: The effect of solution composition on glass dissolution rates. Journal of the American Ceramic Society **96**(8), 2467-2475 (2013). doi:10.1111/jace.12480
164. Hanein, T., Galan, I., Glasser, F.P., Skalamprinos, S., Elhoweris, A., Imbabi, M.S., Bannerman, M.N.: Stability of ternesite and the production at scale of ternesite-based clinkers. Cement and Concrete Research **98**, 91-100 (2017). doi:https://doi.org/10.1016/j.cemconres.2017.04.010
165. Yliniemi, J., Walkley, B., Provis, J.L., Kinnunen, P., Illikainen, M.: Nanostructural evolution of alkali-activated mineral wools. Cement and Concrete Composites **106**, 103472 (2020). doi:https://doi.org/10.1016/j.cemconcomp.2019.103472
166. Ke, X., Criado, M., Provis, J.L., Bernal, S.A.: Slag-based cements that resist damage induced by carbon dioxide. ACS Sustainable Chemistry & Engineering **6**(4), 5067-5075 (2018). doi:10.1021/acssuschemeng.7b04730
167. Bernal, S.A., San Nicolas, R., Myers, R.J., Mejía de Gutiérrez, R., Puertas, F., van Deventer, J.S.J., Provis, J.L.: Mgo content of slag controls phase evolution and structural changes

induced by accelerated carbonation in alkali-activated binders. Cement and Concrete Research **57**, 33-43 (2014). doi:http://dx.doi.org/10.1016/j.cemconres.2013.12.003
168. Mindess, S.: Resistance of concrete to destructive agencies. In: Hewlett, P.C., Liska, M. (eds.) Lea's chemistry of cement and concrete. (2019)
169. Bernal, S.A., Provis, J.L., Brice, D.G., Kilcullen, A., Duxson, P., van Deventer, J.S.J.: Accelerated carbonation testing of alkali-activated binders significantly underestimates service life: The role of pore solution chemistry. Cement and Concrete Research **42**(10), 1317-1326 (2012). doi:http://dx.doi.org/10.1016/j.cemconres.2012.07.002
170. Vichit-Vadakan, W., Scherer, G.W.: Measuring permeability and stress relaxation of young cement paste by beam bending. Cement and Concrete Research **33**(12), 1925-1932 (2003). doi:10.1016/s0008-8846(03)00168-6
171. Williams, R.P., Hart, R.D., van Riessen, A.: Quantification of the extent of reaction of metakaolin-based geopolymers using x-ray diffraction, scanning electron microscopy, and energy-dispersive spectroscopy. Journal of the American Ceramic Society **94**(8), 2663-2670 (2011).
172. White, C.E., Provis, J.L., Bloomer, B., Henson, N.J., Page, K.: In situ x-ray pair distribution function analysis of geopolymer gel nanostructure formation kinetics. Physical Chemistry Chemical Physics **15**(22), 8573-8582 (2013).
173. Gong, K., Cheng, Y., Daemen, L.L., White, C.E.: *In situ* quasi-elastic neutron scattering study on the water dynamics and reaction mechanisms in alkali-activated slags. Physical Chemistry Chemical Physics **21**(20), 10277-10292 (2019). doi:10.1039/C9CP00889F
174. Criado, M., Fernández-Jiménez, A., de la Torre, A.G., Aranda, M.A.G., Palomo, A.: An xrd study of the effect of the sio2/na2o ratio on the alkali activation of fly ash. Cement and Concrete Research **37**, 671-679 (2007).
175. Yang, K., White, C.E.: Modeling the formation of alkali aluminosilicate gels at the mesoscale using coarse-grained monte carlo. Langmuir **32**(44), 11580–11590 (2016). doi:10.1021/acs.langmuir.6b02592
176. Glasser, F.P., Marchand, J., Samson, E.: Durability of concrete — degradation phenomena involving detrimental chemical reactions. Cement and Concrete Research **38**(2), 226-246 (2008). doi:http://dx.doi.org/10.1016/j.cemconres.2007.09.015
177. Lothenbach, B., Scrivener, K., Hooton, R.D.: Supplementary cementitious materials. Cement and Concrete Research **41**(12), 1244-1256 (2011). doi:https://doi.org/10.1016/j.cemconres.2010.12.001
178. Shi, Z., Ferreiro, S., Lothenbach, B., Geiker, M.R., Kunther, W., Kaufmann, J., Herfort, D., Skibsted, J.: Sulfate resistance of calcined clay - limestone - portland cements. Cement and Concrete Research **116**, 238-251 (2019). doi:https://doi.org/10.1016/j.cemconres.2018.11.003
179. Puertas, F., Fernández-Jiménez, A., Blanco-Varela, M.T.: Pore solution in alkali-activated slag cement pastes. Relation to the composition and structure of calcium silicate hydrate. Cement and Concrete Research **34**(1), 139-148 (2004).
180. Lloyd, R.R., Provis, J.L., van Deventer, J.S.J.: Pore solution composition and alkali diffusion in inorganic polymer cement. Cement and Concrete Research **40**(9), 1386-1392 (2010).
181. Nedeljković, M., Ghiassi, B., van der Laan, S., Li, Z., Ye, G.: Effect of curing conditions on the pore solution and carbonation resistance of alkali-activated fly ash and slag pastes. Cement and Concrete Research **116**, 146-158 (2019). doi:https://doi.org/10.1016/j.cemconres.2018.11.011
182. Lothenbach, B., Winnefeld, F., Alder, C., Wieland, E., Lunk, P.: Effect of temperature on the pore solution, microstructure and hydration products of portland cement pastes. Cement and Concrete Research **37**(4), 483-491 (2007). doi:http://dx.doi.org/10.1016/j.cemconres.2006.11.016
183. Han, S.-J., Yoo, M., Kim, D.-W., Wee, J.-H.: Carbon dioxide capture using calcium hydroxide aqueous solution as the absorbent. Energy & Fuels **25**, 3825-3834 (2011).

184. Lucile, F., Cézac, P., Contamine, F., Serin, J.-P., Houssin, D., Arpentinier, P.: Solubility of carbon dioxide in water and aqueous solution containing sodium hydroxide at temperatures from (293.15 to 393.15) k and pressure up to 5 mpa: Experimental measurements. Journal of Chemical & Engineering Data **57**(3), 784-789 (2012). doi:10.1021/je200991x
185. Bernal, S.A., Rose, V., Provis, J.L.: The fate of iron in blast furnace slag particles during alkali-activation. Mater. Chem. Phys. **146**(1-2), 1-5 (2014). doi:10.1016/j.matchemphys.2014.1003.1017
186. Pan, X., Shi, C., Zhang, J., Jia, L., Chong, L.: Effect of inorganic surface treatment on surface hardness and carbonation of cement-based materials. Cement and Concrete Composites **90**, 218-224 (2018). doi:https://doi.org/10.1016/j.cemconcomp.2018.03.026
187. Li, Q., Yang, Y., Yang, K., Chao, Z., Tang, D., Tian, Y., Wu, F., Basheer, M., Yang, C.: The role of calcium stearate on regulating activation to form stable, uniform and flawless reaction products in alkali-activated slag cement. Cement and Concrete Composites **103**, 242-251 (2019). doi:https://doi.org/10.1016/j.cemconcomp.2019.05.009
188. Balonis, M., Sant, G., Burkan Isgor, O.: Mitigating steel corrosion in reinforced concrete using functional coatings, corrosion inhibitors, and atomistic simulations. Cement and Concrete Composites **101**, 15-23 (2019). doi:https://doi.org/10.1016/j.cemconcomp.2018.08.006
189. Criado, M., Bernal, S.A., Garcia-Triñanes, P., Provis, J.L.: Influence of slag composition on the stability of steel in alkali-activated cementitious materials. Journal of Materials Science **53**(7), 5016-5035 (2018). doi:10.1007/s10853-017-1919-3
190. Criado, M., Provis, J.L.: Alkali activated slag mortars provide high resistance to chloride-induced corrosion of steel. Frontiers in Materials **5**, 34 (2018). doi:10.3389/fmats.2018.00034
191. Neville, A.: Chloride attack of reinforced concrete: An overview. Materials and Structures **28**(2), 63 (1995). doi:10.1007/BF02473172
192. Li, K., Li, L.: Crack-altered durability properties and performance of structural concretes. Cement and Concrete Research **124**, 105811 (2019). doi:https://doi.org/10.1016/j.cemconres.2019.105811
193. Walling, S.A., Provis, J.L.: Magnesia-based cements: A journey of 150 years, and cements for the future? Chemical Reviews **116**(7), 4170-4204 (2016). doi:10.1021/acs.chemrev.5b00463
194. Iyengar, S.R., Al-Tabbaa, A.: Developmental study of a low-ph magnesium phosphate cement for environmental applications. Environmental Technology **28**(12), 1387-1401 (2007). doi:10.1080/09593332808618899
195. Sharkawi, A.E., Rizkala, S., Zia, P.: Corrosion activity of steel bars embedded in magnesium phosphate fiber reinforced cementitious material “pcw grancrete”. In: American society of civil engineers 6th international engineering and construction conference (iecc’6). Cairo, Egypt (2010)
196. Subramanian, N.: Sustainability of rcc structures using basalt composite rebars. The Masterbuilder (2010).
197. Dhand, V., Mittal, G., Rhee, K.Y., Park, S.-J., Hui, D.: A short review on basalt fiber reinforced polymer composites. Composites Part B: Engineering **73**, 166-180 (2015). doi:https://doi.org/10.1016/j.compositesb.2014.12.011
198. Inman, M., Thorhallsson, E.R., Azrague, K.: A mechanical and environmental assessment and comparison of basalt fibre reinforced polymer (bfrp) rebar and steel rebar in concrete beams. Energy Procedia **111**, 31-40 (2017). doi:https://doi.org/10.1016/j.egypro.2017.03.005
199. Antonopoulou, S., McNally, C., Byrne, G.: Development of braided basalt frp rebar for reinforcement of concrete structures. In: 8th international conference on fibre-reinforced polymer (frp) composites in civil engineering (cice 2016). Hong Kong (2016)
200. Ding, Z., Lu, Z.X., Li, Y.: Feasibility of basalt fiber reinforced inorganic adhesive for concrete strengtening. Advanced Materials Research **287-290**, 1197-1200 (2011). doi:10.4028/www.scientific.net/AMR.287-290.1197

201. Urbanski, M., Lapko, A., Garbacz, A.: Investigation on concrete beams reinforced with basalt rebars as an effective alternative of conventional r/c structures. Procedia Engineering **57**, 1183-1191 (2013). doi:https://doi.org/10.1016/j.proeng.2013.04.149
202. Lapko, A., Urbański, M.: Experimental and theoretical analysis of deflections of concrete beams reinforced with basalt rebar. Archives of Civil and Mechanical Engineering **15**(1), 223-230 (2015). doi:https://doi.org/10.1016/j.acme.2014.03.008
203. Duic, J., Kenno, S., Das, S.: Performance of concrete beams reinforced with basalt fibre composite rebar. Construction and Building Materials **176**, 470-481 (2018). doi:https://doi.org/10.1016/j.conbuildmat.2018.04.208
204. Elavenil, S., Saravanan, S., Reddy, R.: Investigation of structural members with basalt rebar reinforcement as effective alternative of standard steel rebar. Journal of Industrial Pollution Control **33**(S3), 1422-1429 (2017).
205. Tomlinson, D., Fam, A.: Performance of concrete beams reinforced with basalt frp for flexure and shear. Journal of Composites for Construction **19**(2), 04014036 (2015). doi:10.1061/(ASCE)CC.1943-5614.0000491
206. Bang, J.W., Prabhu, G.G., Jang, Y.I., Kim, Y.Y.: Development of ecoefficient engineered cementitious composites using supplementary cementitious materials as a binder and bottom ash aggregate as fine aggregate. International Journal of Polymer Science, 681051 (2015).
207. Cai, J., Pan, J., Zhou, X.: Flexural behavior of basalt frp reinforced ecc and concrete beams. Construction and Building Materials **142**, 423-430 (2017). doi:https://doi.org/10.1016/j.conbuildmat.2017.03.087
208. Fan, X., Zhang, M.: Behaviour of inorganic polymer concrete columns reinforced with basalt frp bars under eccentric compression: An experimental study. Composites Part B: Engineering **104**, 44-56 (2016). doi:https://doi.org/10.1016/j.compositesb.2016.08.020
209. Serbescu, A., Guadagnini, M., Pilakoutas, K.: Mechanical characterization of basalt frp rebars and long-term strength predictive model. Journal of Composites for Construction **19**(2), 04014037 (2015). doi:10.1061/(ASCE)CC.1943-5614.0000497
210. John, V.M., Quattrone, M., Abrão, P.C.R.A., Cardoso, F.A.: Rethinking cement standards: Opportunities for a better future. Cement and Concrete Research **124**, 105832 (2019). doi:https://doi.org/10.1016/j.cemconres.2019.105832
211. van Deventer, J.S.J., Provis, J.L., Duxson, P.: Technical and commercial progress in the adoption of geopolymer cement. Minerals Engineering **29**, 89-104 (2012). doi:10.1016/j.mineng.2011.09.009
212. Van Deventer, J.S.J., Brice, D.G., Bernal, S.A., Provis, J.L.: Development, standardization and applications of alkali-activated concretes. In: Struble, L., Hicks, J.K. (eds.) Astm symposium on geopolymer binder systems, special technical paper 1566. California, United States (2013)
213. Provis, J.L., van Deventer, J.S.J. (eds.): Alkali-activated materials. Springer/RILEM, Dordrecht, Netherlands (2014)
214. Van Deventer, J.S.J., Provis, J.L.: Low carbon emission geopolymer concrete: From research into practice. In: 27th biennial national conference of the concrete institute of australia in conjunction with the 69th rilem week. Melbourne, Australia (2015)
215. San Nicolas, R.V.R., Walkley, B., van Deventer, J.S.J.: 7 - fly ash-based geopolymer chemistry and behavior. In: Robl, T., Oberlink, A., Jones, R. (eds.) Coal combustion products (ccp's). pp. 185-214. Woodhead Publishing, (2017)
216. Alexander, M., Thomas, M.: Service life prediction and performance testing — current developments and practical applications. Cement and Concrete Research **78**, 155-164 (2015). doi:https://doi.org/10.1016/j.cemconres.2015.05.013
217. Beushausen, H., Torrent, R., Alexander, M.G.: Performance-based approaches for concrete durability: State of the art and future research needs. Cement and Concrete Research **119**, 11-20 (2019). doi:https://doi.org/10.1016/j.cemconres.2019.01.003

218. Hooton, D.R.: Future directions for design, specification, testing, and construction of durable concrete structures. Cement and Concrete Research **124**, 105827 (2019). doi:https://doi.org/10.1016/j.cemconres.2019.105827